Organometallic 3-(1H-Benzimidazol-2-yl)-1H-pyrazolo-[3,4-b]pyridines as Potential Anticancer Agents

Iryna N. Stepanenko, Maria S. Novak, Gerhard Mühlgassner, Alexander Roller, Michaela Hejl, Vladimir B. Arion,* Michael A. Jakupec, and Bernhard K. Keppler*

University of Vienna, Institute of Inorganic Chemistry, Währinger Strasse 42, A-1090 Vienna, Austria

S *Supporting Information*

ABSTRACT: Six organometallic complexes of the general formula $[M^{II}Cl(\eta^6\text{-}p\text{-cymene})(L)]Cl$, where M = Ru (**11a**, **12a**, **13a**) or Os (**11b**, **12b**, **13b**) and L = 3-(1H-benzimidazol-2-yl)-1H-pyrazolo-[3,4-b]pyridines (**L1**−**L3**) have been synthesized. The latter are known as potential cyclin-dependent kinase (Cdk) inhibitors. All compounds have been comprehensively characterized by elemental analysis, one- and two-dimensional NMR spectroscopy, UV−vis spectroscopy, ESI mass spectrometry, and X-ray crystallography (**11b** and **12b**). The multistep synthesis of 3-(1H-benzimidazol-2-yl)-1H-pyrazolo[3,4-b]pyridines (**L1**−**L3**), which was reported by other researchers, has been modified by us essentially (e.g., the synthesis of 5-bromo-1H-pyrazolo[3,4-b]pyridine-3-carboxylic acid (**3**) via 5-bromo-3-methyl-1H-pyrazolo[3,4-b]pyridine (**2**); the synthesis of 1-methoxymethyl-2,3-diaminobenzene (**5**) by avoiding the use of unstable 2,3-diaminobenzyl alcohol; and the activation of 1H-pyrazolo[3,4-b]pyridine-3-carboxylic acids (**1**, **3**) through the use of an inexpensive coupling reagent, N,N'-carbonyldiimidazole (CDI)). Stabilization of the 7b tautomer of methoxymethyl-substituted **L3** by coordination to a metal(II) center, as well as the NMR spectroscopic characterization of two tautomers 7b-**L3** and 4b'-**L3** in a metal-free state are described. Structure−activity relationships with regard to cytotoxicity and cell cycle effects in human cancer cells, as well as Cdk inhibitory activity, are also reported.
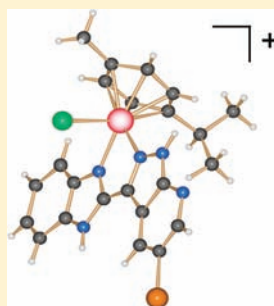
New candidates for metal-based targeted chemotherapy?

■ INTRODUCTION

Tumor-associated cell cycle defects, manifesting in unscheduled proliferation, and the associated genomic and chromosomal instabilities are mediated by misregulation of cyclin-dependent kinases (Cdks).[1] Because of the main role in the division cycle, Cdks have been recognized as targets for anticancer therapy. Many small-molecule organic compounds, which have been identified as Cdk modulators, are currently in preclinical or clinical development.[1−5] However, no Cdk inhibitors have gained marketing approval, despite 20 years of scientific investigation.[1]

Several studies have shown synergism when Cdk inhibitors were combined with organic (e.g., doxorubicin, paclitaxel)[2,6] and inorganic (e.g., cisplatin, carboplatin) cytotoxic drugs.[7−9] The reported effects inspired the design of metal complexes with biologically active ligands. The first publications have appeared recently and include Fe, Cu, and Pt complexes with Cdk inhibitors derived from 6-benzylaminopurine,[10−13] metal-based indolo-[3,2-d]benzazepines (paullones; Ga, Cu, Ru, and Os),[14−19] and indolo-[3,2-c]quinolines (Ru, Os).[20]

Another class of compounds potentially suitable for targeted metal-based chemotherapy is that of 3-(1H-benzimidazol-2-yl)-1H-pyrazolo[3,4-b]pyridines. These have been documented recently as potent Cdk1 inhibitors with antiproliferative activity in HeLa (cervical carcinoma), HCT116 (colon carcinoma), and A375 (melanoma) human cancer cell lines.[21−23] Comparison of

Cdk1 inhibitory activity with the inhibiting activity in four other protein kinases (VEGF-R2, HER2, Aurora-A, and RET) revealed selectivity for Cdk1. Structural modifications consisting of a replacement of both bicyclic rings in 3-(1H-benzimidazol-2-yl)-1H-pyrazolo[3,4-b]pyridines by monocycles while retaining the imidazolyl pyrazole core have been proposed in order to obtain inhibitors with improved pharmacokinetic and solubility properties.[24−26] The most promising were suggested to be 3-(1H-benzimidazol-2-yl)-1H-pyrazolo[3,4-b]pyridines (see Chart 1). The inspection of substitution patterns on the benzimidazole moiety and structure−activity relationships revealed that a methoxymethyl group in position 7b (4b') is favorable for Cdk1 inhibiting potency. The role of the pyrazole NH group is also of note, since its methylation led to a significant reduction of Cdk1 activity. The effect of various heteroaryl groups in position 5a was also remarkable for the development of more-effective Cdk inhibitors and antiproliferative agents.

Our previous experience with metal-based indolo-[3,2-d]benzazepines prompted the use of the half-sandwich metal-arene moiety as a suitable scaffold to which 3-(1H-benzimidazol-2-yl)-1H-pyrazolo[3,4-b]pyridines may be attached. Organometallic compounds $[M(\eta^6\text{-arene})(YZ)X]^n$ (where M = Ru, Os) exhibit

Chart 1. Compounds Reported in This Work with Atom Numbering Schemes for NMR Signal Assignment[a]
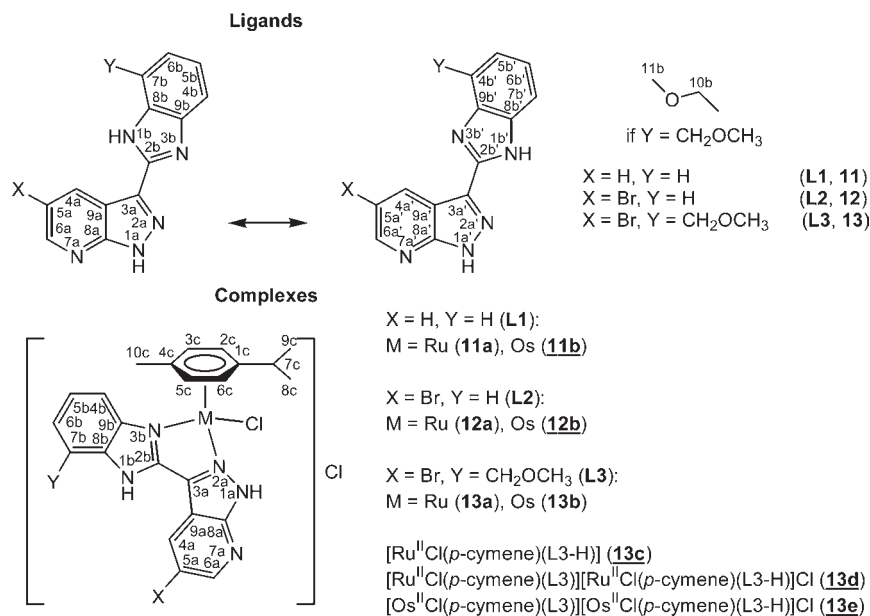
^{a}Underlined compounds have been characterized by X-ray diffraction (XRD).

promising anticancer activity and are the focus of attention for several groups.[27−32] These compounds have shown activity toward classic (DNA) and nonclassic (e.g., Cdks) targets in anticancer chemotherapy.

Herein, we report (i) the modified synthetic approach to 3-(1H-benzimidazol-2-yl)-1H-pyrazolo[3,4-b]pyridines (recall Chart 1: **L1**, X = H, Y = H; **L2**, X = Br; Y = H; **L3**, X = Br; Y = CH₂OCH₃); (ii) the synthesis and characterization of a new family of organoruthenium(II) (**11a**, **12a**, **13a**) and osmium(II) (**11b**, **12b**, **13b**) complexes of the general formula [MCl(η^6-p-cymene)L]Cl, where L = 3-(1H-benzimidazol-2-yl)-1H-pyrazolo-[3,4-b]pyridines (**L1**−**L3**) (Chart 1); (iii) stabilization of the 7b tautomer of methoxymethyl-substituted **L3** by metal coordination as well as (iv) NMR spectroscopic characterization of two tautomers 7b-**L3** and 4b′-**L3** in a metal-free state; and (v) cell cycle effects, as well as the antiproliferative and Cdk inhibitory activities of both metal-free ligands and organometallic complexes.

■ EXPERIMENTAL SECTION

Starting Materials. 3-Acetyl-2-chloropyridine and 3-methyl-1H-pyrazolo[3,4-b]pyridine were prepared according to literature protocols.[33−35] 1H-Pyrazolo[3,4-b]pyridine-3-carboxylic acid (**1**) was obtained via the oxidation of 3-methyl-1H-pyrazolo[3,4-b]pyridine by KMnO₄ in the presence of a base,[35] followed by acidification with 37% HCl. 2-Amino-3-nitrobenzyl alcohol was obtained as reported in the literature.[36] 1, 2-Diaminobenzene and dry dimethylformamide (DMF) were purchased from Acros Organics. Solvents [toluene, ethanol (EtOH), tetrahydrofuran (THF), diethyl ether (Et₂O)] were dried using standard procedures. [Ru^{II}Cl(μ-Cl)(η^6-p-cymene)]₂ and [Os^{II}Cl(μ-Cl)(η^6-p-cymene)]₂ were synthesized as described previously.[37,38]

Synthesis of Ligands. *5-Bromo-3-methyl-1H-pyrazolo[3,4-b]-pyridine (2).* 3-Methyl-1H-pyrazolo[3,4-b]pyridine (10.9 g, 0.08 mol) and anhydrous sodium acetate (10.21 g, 0.13 mol) were suspended in glacial acetic acid (42 mL). Bromine (20.42 g, 0.13 mol) was added,

and the resulting mixture was stirred at room temperature for 2−2.5 h and then at 110−115 °C for 2.5−3 h. Afterward, water (300−350 mL) was added and the mixture was stirred at room temperature. The formed light yellow precipitate was filtered off and dried in vacuo at 40−50 °C. Yield: 17 g. The raw product was used without further purification in the next step. Purification by column chromatography afforded a white powder (SiO₂, EtOAc, R$_f$ = 0.79; 12.5 g, 72.6% yield). M_r (C₇H₆BrN₃) = 212.05 g/mol. ESI-MS in MeOH (positive): m/z 213 [M+H]⁺, 235 [M+Na]⁺, 253 [M+K]⁺; (negative): m/z 211 [M−H]⁻. ¹H NMR (500.32 MHz, MeOH-d_4): δ 8.55 (d, 1H, J = 2.16 Hz, CH), 8.43 (d, 1H, J = 2.15 Hz, CH), 2.56 (s, 3H, CH₃) ppm. ¹H NMR (500.32 MHz, DMSO-d_6): δ 13.42 (brs, 1H, NH), 8.54 (d, 1H, J = 2.19 Hz, CH), 8.53 (d, 1H, J = 2.18 Hz, CH), 2.49 (s, 3H, CH₃) ppm. Colorless crystals of **2**·0.5H₂O suitable for X-ray diffraction (XRD) study were grown in EtOAc (see Figure S1 in the Supporting Information).

5-Bromo-1H-pyrazolo[3,4-b]pyridine-3-carboxylic acid (3). To sodium hydroxide (9.54 g, 0.24 mol) in water (150 mL) was added the raw product **2** (7.1 g, 0.03 mol). After a dropwise addition of KMnO₄ (16.98 g, 0.11 mol) in water (300 mL) at 100 °C over 2 h, the reaction mixture was further heated for 1 h. MnO₂ was filtered off from the hot reaction mixture and washed with hot water. The filtrates were combined, the water was evaporated to ca. 400 mL, and the yellow solution was acidified to pH ∼2, using concentrated HCl. The yellow precipitate was filtered off and dried in vacuo at 60 °C. Yield: 2.28 g. The crude hydrochloride of **3** was used without further purification in the next step. M_r(C₇H₄BrN₃O₂) = 242.03 g/mol. ESI-MS in MeOH (positive): m/z 243 [M+H]⁺, 265 [M+Na]⁺, 287 [M+2Na−H]⁺; (negative): m/z 241 [M−H]⁻. ¹H NMR (500.32 MHz, MeOH-d_4): δ 8.69 (d, 1H, J = 2.22 Hz, CH), 8.68 (d, 1H, J = 2.22 Hz, CH) ppm. ¹H NMR (500.32 MHz, DMSO-d_6): δ 14.65 (s, 1H, NH), 13.45 (brs, 1H, NH), 8.72 (d, 1H, J = 2.23 Hz, CH), 8.58 (d, 1H, J = 2.25 Hz, CH) ppm.

1-Methoxymethyl-2-amino-3-nitrobenzene (4). NaH (1.75 g, 0.07 mol) was suspended in dry THF (200 mL). A solution of 2-amino-3-nitrobenzyl alcohol (5.23 g, 0.03 mol) in dry THF (100 mL) was added dropwise at 0 °C and the mixture was stirred at the same temperature for 15 min. After a dropwise addition of MeI (11.5 g, 0.08 mol), stirring was continued at room

11716

dx.doi.org/10.1021/ic201704u |*Inorg. Chem.* 2011, 50, 11715−11728

temperature for 3 h. A saturated aqueous solution of $NaHCO_3$ (300 mL) and MeOH (300 mL) then were added. The mixture was filtered, and the white precipitate was washed with EtOAc. The filtrates were combined, and organic solvents were evaporated under reduced pressure. The remaining aqueous solution was extracted with EtOAc (2 × 300 mL). The organic phase was dried over Na_2SO_4, filtered, and evaporated to yield a red oil (4.85 g). The raw product was purified by column chromatography (SiO_2, EtOAc, or EtOAc/hexane 1/1, first fraction, a red-orange oil crystallized to form a red solid at 4 °C; yield: 3.68 g, 65%). M_r ($C_8H_{10}N_2O_3$) = 182.18 g/mol. ^1H NMR (500.32 MHz, DMSO-d_6): δ 8.00 (d, 1H, J = 8.71 Hz, C_6H_3), 7.48 (d, 1H, J = 7.1 Hz, C_6H_3), 7.09 (br, 2H, NH_2), 6.67 (t, 1H, J = 8.45 Hz, C_6H_3), 4.48 (s, 2H, CH_2), 3.31 (s, 3H, CH_3) ppm.

1-Methoxymethyl-2,3-diaminobenzene (**5**). A mixture of **4** (1.4 g, 0.008 mol) and 10% Pd/C (0.18 g) in dry EtOH (55 mL) was stirred under hydrogen atmosphere at room temperature for 18−24 h. The catalyst was removed by filtration through GF-3-filter under argon and washed with dry EtOH (50−70 mL). The filtrate was evaporated in vacuo to give a light-orange solid (1.17 g, 100% yield), which was used immediately in the next step. M_r($C_8H_{12}N_2O$) = 152.19 g/mol. ^1H NMR (500.32 MHz, DMSO-d_6): δ 6.52 (dd, 1H, J = 1.87 Hz, J = 7.25, C_6H_3), 6.42−6.36 (m, 2H, C_6H_3), 4.48 (br, 2H, NH_2), 4.31 (br, 4H, NH_2+CH_2), 3.24 (s, 3H, CH_3) ppm.

(1H-Imidazol-1-yl)(1H-pyrazolo[3,4-b]pyridin-3-yl)methanone (**6**). N,N'-Carbonyldiimidazole (CDI, 4.16 g, 0.026 mol) was added in small portions to **1** (2.34 g) in dry DMF (12 mL). The mixture was stirred at room temperature for 20−24 h. Water (5 mL) then was added and the suspension was stirred until all CO_2 was ceased. The white precipitate was filtered off, washed with water (3−5 mL), and dried in a sublimator in vacuo at 60 °C, to remove the imidazole as a contaminant. Yield: 1.13 g; 25−29%, based on 3-methyl-1H-pyrazolo[3,4-b]pyridine. M_r ($C_{10}H_7N_5O$) = 213.19 g/mol. ESI-MS in methanol (positive): m/z 214 $[M+H]^+$, 237 $[M+Na]^+$; (negative): m/z 212 $[M−H]^-$. ^1H NMR (500.32 MHz, DMSO-d_6): δ 14.95 (brs, 1H, NH), 8.91 (s, 1H, CH_{im}), 8.74 (dd, 1H, J = 1.61 Hz, J = 4.51 Hz, CH_{py}), 8.63 (dd, 1H, J = 1.59 Hz, J = 8.12 Hz, CH_{py}), 8.14 (t, 1H, J = 1.23 Hz, CH_{im}), 7.51 (dd, 1H, J = 4.46 Hz, J = 8.06 Hz, CH_{py}), 7.20 (s, 1H, CH_{im}) ppm.

(5-Bromo-1H-pyrazolo[3,4-b]pyridin-3-yl)(1H-imidazol-1-yl)methanone (**7**). N,N'-Carbonyldiimidazole (CDI, 16.2 g, 0.1 mol) was added in small portions to crude **3** (11.58 g) in dry DMF (70 mL). The mixture was stirred at room temperature for 20−24 h. Water (10 mL) then was added and the suspension was stirred until all CO_2 was ceased. The white precipitate was filtered off, washed with water (10−15 mL), and dried in a sublimator in vacuo at 60 °C, to remove the imidazole as a contaminant. Yield: 7.27 g, 13−16%, based on 3-methyl-1H-pyrazolo[3,4-b]-pyridine. M_r($C_{10}H_6BrN_5O$) = 292.09 g/mol. ESI-MS in methanol (positive): m/z 315 $[M+Na]^+$; (negative): m/z 291 $[M−H]^-$. ^1H NMR (500.32 MHz, DMSO-d_6): δ 14.95 (brs, 1H, NH), 8.89 (s, 1H, CH_{im}), 8.83 (d, 1H, J = 2.12 Hz, CH_{py}), 8.75 (d, 1H, J = 2.07 Hz, CH_{py}), 8.13 (s, 1H, CH_{im}), 7.20 (s, 1H, CH_{im}) ppm.

N-(2-Aminophenyl)-1H-pyrazolo[3,4-b]pyridine-3-carboxamide (**8**). The solution of 1,2-diaminobenzene (0.5 g, 4.67 mmol) in dry DMF (2 mL) was added to the suspension of **6** (0.94 g, 4.41 mmol) in dry DMF (13 mL), and this reaction mixture was heated under argon at 85 °C for 5 h. DMF then was evaporated in vacuo at 50 °C and water (10−12 mL) was added. The light-yellow precipitate was filtered off and dried in vacuo at 50 °C. Yield: 0.86 g. The raw product was used without purification in the next step. M_r-($C_{13}H_{11}N_5O$) = 253.26 g/mol. ESI-MS in methanol (positive): m/z 255 $[M+H]^+$, 277 $[M+Na]^+$; (negative): m/z 253 $[M−H]^-$. ^1H NMR (500.32 MHz, DMSO-d_6): δ 14.30 (brs, 1H, NH_{pz}), 9.73 (brs, 1H, CONH), 8.64 (dd, 1H, J = 1.59 Hz, J = 4.44 Hz, CH_{py}), 8.56 (dd, 1H, J = 1.53 Hz, J = 8.02 Hz, CH_{py}), 7.39−7.36 (m, 2H, CH_{py}+CH_{bz}), 6.97 (td, 1H, J = 1.31 Hz, J = 7.73 Hz, CH_{bz}), 6.82

(dd, 1H, J = 1.2 Hz, J = 7.89 Hz, CH_{bz}), 6.64 (td, 1H, J = 1.2 Hz, J = 7.67 Hz, CH_{bz}), 4.93 (s, 2H, NH_2) ppm.

N-(2-Aminophenyl)-5-bromo-1H-pyrazolo[3,4-b]pyridine-3-carboxamide (**9**). The solution of 1,2-diaminobenzene (0.96 g, 8.88 mmol) in dry DMF (10 mL) was added to the suspension of **7** (2.28 g, 7.8 mmol) in dry DMF (10 mL), and this mixture was heated under argon at 85 °C for 7 h. DMF then was evaporated in vacuo at 50 °C and water (20 mL) was added. The yellow precipitate was filtered off and dried in vacuo at 50 °C. Yield: ∼2.2 g. The raw product was used without purification in the next step. M_r($C_{13}H_{10}BrN_5O$) = 332.16 g/mol. ESI-MS in methanol (positive): m/z 333 $[M+H]^+$, 355 $[M+Na]^+$; (negative): m/z 331 $[M−H]^-$. ^1H NMR (500.32 MHz, DMSO-d_6): δ 14.54 (brs, 1H, NH_{pz}), 9.80 (brs, 1H, CONH), 8.73 (d, 1H, J = 2.26 Hz, CH_{py}), 8.69 (d, 1H, J = 2.22 Hz, CH_{py}), 7.34 (dd, 1H, J = 0.98 Hz, J = 7.88 Hz, CH_{bz}), 6.99 (td, 1H, J = 1.43 Hz, J = 8.03 Hz, CH_{bz}), 6.82 (dd, 1H, J = 1.22 Hz, J = 7.96 Hz, CH_{bz}), 6.64 (td, 1H, J = 1.19 Hz, J = 7.73 Hz, CH_{bz}), 4.94 (s, 2H, NH_2) ppm.

N-[2-Amino-3-(methoxymethyl)phenyl]-5-bromo-1H-pyrazolo-[3,4-b]pyridine-3-carboxamide (**10**). A mixture of **5** (1.17 g, 7.69 mmol) and **7** (2.1 g, 7.2 mmol) in dry DMF (45 mL) was heated under argon at 85 °C for 20 h. DMF then was evaporated in vacuo at 50 °C and water (20 mL) was added. The brown precipitate formed was filtered off and dried in vacuo at 50 °C. Yield: ∼2.3 g. The product was used without further purification in the next step. M_r($C_{15}H_{14}BrN_5O_2$) = 376.21 g/mol. ESI-MS in methanol (positive): m/z 399 $[M+Na]^+$; (negative): m/z 375 $[M−H]^-$. ^1H NMR (500.32 MHz, DMSO-d_6): δ 14.54 (brs, 1H, NH_{pz}), 9.85 (brs, 1H, CONH), 8.73 (d, 1H, J = 2.13 Hz, CH_{py}), 8.68 (d, 1H, J = 2.05 Hz, CH_{py}), 7.29 (d, 1H, J = 7.56 Hz, CH_{bz}), 7.03 (d, 1H, J = 7.29 Hz, CH_{bz}), 6.65 (t, 1H, J = 7.79 Hz, CH_{bz}), 4.78 (brs, 2H, NH_2), 4.42 (s, 2H, CH_2), 3.29 (s, 3H, CH_3) ppm.

3-(1H-Benzimidazol-2-yl)-1H-pyrazolo[3,4-b]pyridine (**11**, **L1**). The raw product **8** (0.86 g) was heated in a glacial acetic acid (10 mL) at 125 °C for 2.5 h. The solvent was evaporated under reduced pressure and the residue was dried in vacuo at 50 °C, then resuspended in CH_2Cl_2/MeOH (4/1, 25 mL), filtered off, and dried in vacuo to give **L1** as a white powder (0.4 g). The filtrate was evaporated and the residue was purified by column chromatography (SiO_2, EtOAc, R_f = 0.58) to give an additional amount of **L1** (0.22 g). Yield: 0.62 g, ∼60% based on **6**. M_r ($C_{13}H_9N_5$) = 235.24 g/mol. Anal. Calcd for **11**·0.15H_2O·0.1 EtOAc (M_r = 246.76 g/mol): C, 65.22; H, 4.13; N, 28.38. Found: C, 65.56; H, 3.90; N, 28.39. ESI-MS in methanol (positive): m/z 237 $[M+H]^+$, 259 $[M+Na]^+$; (negative): m/z 235 $[M−H]^-$. UV−vis (methanol), λ_{max}, nm (ε, M^{-1} cm^{-1}): 232 (25618), 275 (15198), 324 (22333). ^1H NMR (500.32 MHz, DMSO-d_6): δ 14.19 (brs, 1H, H_{1a}), 13.11 (brs, 1H, H_{1b}), 8.85 (dd, 1H, J = 1.5 Hz, J = 8.1 Hz, H_{4a}), 8.66 (dd, 1H, J = 1.5 Hz, J = 4.5 Hz, H_{6a}), 7.75 (d, 1H, J = 7.3 Hz, H_{4b} or H_{7b}), 7.54 (d, 1H, J = 7.7 Hz, H_{4b} or H_{7b}), 7.39 (dd, 1H, J = 4.5 Hz, J = 8.0 Hz, H_{5a}), 7.24 (m, 2H, H_{5b}+H_{6b}) ppm. ^{13}C NMR (125.81 MHz, DMSO-d_6): δ 153.13 (C_{8a}), 150.22 (C_{6a}), 146.99 (C_{2b}), 144.34 (C_{8b} or C_{9b}), 136.06 (C_{3a}), 134.68 (C_{8b} or C_{9b}), 131.82 (C_{4a}), 123.35 (C_{5b} or C_{6b}), 122.11 (C_{5b} or C_{6b}), 119.44 (C_{4b} or C_{7b}), 118.65 (C_{5a}), 113.33 (C_{9a}), 112.01 (C_{4b} or C_{7b}) ppm. ^{15}N NMR (50.70 MHz, DMSO-d_6): δ 166.2 (N_{1a}), 121.3 (N_{1b}) ppm.

3-(1H-Benzimidazol-2-yl)-5-bromo-1H-pyrazolo[3,4-b]pyridine (**12**, **L2**). The raw product **9** (2.2 g) was heated in a glacial acetic acid (30 mL) at 125 °C for 2 h. The solvent was evaporated under reduced pressure, and the residue was dried in vacuo at 50 °C, then resuspended in CH_2Cl_2/MeOH (7/1, 50 mL), filtered off and dried in vacuo to give **L2** as a white powder (1.15 g). The filtrate was evaporated and the residue was purified by column chromatography (SiO_2, EtOAc/hexane 2/1, R_f = 0.6) to give an additional amount of the product (0.27 g). Yield: 1.42 g, ∼58% based on **7**. M_r-($C_{13}H_8BrN_5$) = 314.14 g/mol. Anal. Calcd for **12**·0.25H_2O·0.04EtOAc (M_r = 322.17 g/mol): C, 49.06; H, 2.76; N, 21.74. Found: C, 49.44; H, 2.45; N, 21.59. ESI-MS in methanol (positive): m/z 315 $[M+H]^+$, 337 $[M+Na]^+$;

(negative): m/z 313 [M−H]$^−$. UV−vis (methanol), λ_{max}, nm (ε, M^{-1} cm^{-1}): 234 (28154), 282 (17628), 335 (17198). ^{1}H NMR (500.32 MHz, DMSO-d_6): δ 14.43 (brs, 1H, H$_{1a}$), 13.19 (brs, 1H, H$_{1b}$), 8.99 (d, 1H, J = 2.2 Hz, H$_{4a}$), 8.75 (d, 1H, J = 2.3 Hz, H$_{6a}$), 7.77 (d, 1H, J = 7.9 Hz, H$_{4b}$ or H$_{7b}$), 7.54 (d, 1H, J = 7.9 Hz, H$_{4b}$ or H$_{7b}$), 7.26 (m, 2H, H$_{5b}$+H$_{6b}$) ppm. ^{13}C NMR (125.81 MHz, DMSO-d_6): δ 151.49 (C$_{8a}$), 150.66 (C$_{6a}$), 146.42 (C$_{2b}$), 144.24 (C$_{8b}$ or C$_{9b}$), 135.61 (C$_{3a}$), 134.67 (C$_{8b}$ or C$_{9b}$), 133.35 (C$_{4a}$), 123.54 (C$_{5b}$ or C$_{6b}$), 122.27 (C$_{5b}$ or C$_{6b}$), 119.55 (C$_{4b}$ or C$_{7b}$), 114.87 (C$_{5a}$ or C$_{9a}$), 113.49 (C$_{5a}$ or C$_{9a}$), 112.09 (C$_{4b}$ or C$_{7b}$) ppm. ^{15}N NMR (50.70 MHz, DMSO-d_6): δ 167.5 (N$_{1a}$), 121.3 (N$_{1b}$) ppm.

5-Bromo-3-(4-methoxymethyl-1H-benzimidazol-2-yl)-1H-pyrazolo-[3,4-b]pyridine (13, L3). The raw product **10** (2.3 g) was heated in a glacial acetic acid (40 mL) at 125 °C for 2 h. The solvent was evaporated under reduced pressure, and the residue dried in vacuo at 50 °C. After washing with CH$_2$Cl$_2$ (30 mL), CH$_2$Cl$_2$/MeOH (2/1, 5−7 mL) the gray product was purified by column chromatography (SiO$_2$, EtOAc, R$_f$ = 0.68) to give a white powder (0.9 g). The filtrates were evaporated and the remaining solid was purified by column chromatography to give an additional amount of the product (0.3 g). Yield: 1.2 g, 47%, based on **7**. M_r(C$_{15}$H$_{12}$BrN$_5$O) = 358.19 g/mol. Anal. Calcd for **13**: C, 50.29; H, 3.38; N, 19.55. Found: C, 50.03; H, 3.19; N, 19.19. ESI-MS in methanol (positive): m/z 381 [M+Na]$^+$; (negative): m/z 357 [M−H]$^−$. UV−vis (methanol), λ_{max}, nm (ε, M^{-1} cm^{-1}): 235 (29776), 282 (17544), 337 (16958).

NMR characterization of 7b-L3 and 4b'-L3 tautomers (1/1.3) in DMSO-d_6: ^{1}H NMR (500.32 MHz, DMSO-d_6), 7b-**L3**: δ 14.47 (brs, 1H, H$_{1a}$), 13.25 (brs, 1H, H$_{1b}$), 8.99 or 8.98 (d+d, (1 + 1.3)H, J = 2.3 Hz, H$_{4a}$+H$_{4a'}$), 8.75 (d, (1 + 1.3)H, J = 2.3 Hz, H$_{6a}$+H$_{6a'}$), 7.72 (dd, 1H, J = 1.8 Hz, J = 6.8 Hz, H$_{4b}$), 7.28−7.21 (m, (2 + 2.6)H, H$_{5a}$, H$_{6a}$+H$_{5a'}$, H$_{6a'}$), 4.80 (s, 2H, H$_{10b}$), 3.37 (s, 3H, H$_{11b}$) ppm. ^{1}H NMR (500.32 MHz, DMSO-d_6), 4b'-**L3**: δ 14.43 (brs, 1.3H, H$_{1a'}$), 13.22 (brs, 1.3H, H$_{1b'}$), 8.99 or 8.98 (d+d, (1 + 1.3)H, J = 2.3 Hz, H$_{4a}$+H$_{4a'}$), 8.75 (d, (1 + 1.3)H, J = 2.3 Hz, H$_{6a}$+H$_{6a'}$), 7.47 (dd, 1.3H, J = 1.2 Hz, J = 7.7 Hz, H$_{7b'}$), 7.28−7.21 (m, (2 + 2.6)H, H$_{5a}$, H$_{6a}$+H$_{5a'}$, H$_{6a'}$), 4.96 (s, 2.6H, H$_{10b'}$), 3.44 (s, 3.9H, H$_{11b'}$) ppm. ^{13}C NMR (125.81 MHz, DMSO-d_6), 7b-**L3**: δ 151.51 (C$_{8a}$+C$_{8a'}$), 150.69 (C$_{6a}$ or C$_{6a'}$), 150.65 (C$_{6a}$ or C$_{6a'}$), 146.70 (C$_{2b}$), 144.46 (C$_{9b}$), 135.62 (C$_{3a}$+C$_{3a'}$), 133.45 (C$_{4a}$ or C$_{4a'}$), 133.42 (C$_{4a}$ or C$_{4a'}$), 133.29 (C$_{8b}$), 123.38 (C$_{6b}$; C$_{5b}$ or C$_{6b'}$), 123.36 (C$_{6b}$; C$_{5b}$ or C$_{6b'}$), 122.95 (C$_{7b}$), 122.16 (C$_{5b}$ or C$_{6b'}$), 118.97 (C$_{4b}$), 115.04 (C$_{5a}$ or C$_{9a}$ or C$_{5a'}$ or C$_{9a'}$), 114.92 (C$_{5a}$ or C$_{9a}$ or C$_{5a'}$ or C$_{9a'}$), 113.49 (C$_{5a}$ or C$_{9a}$ or C$_{5a'}$ or C$_{9a'}$), 70.49 (C$_{10b}$), 57.95 (C$_{11b}$) ppm. ^{13}C NMR (125.81 MHz, DMSO-d_6), 4b'-**L3**: δ 151.51 (C$_{8a}$+C$_{8a'}$), 150.69 (C$_{6a}$ or C$_{6a'}$), 150.65 (C$_{6a}$ or C$_{6a'}$), 146.13 (C$_{2b'}$), 142.50 (C$_{9b'}$), 135.62 (C$_{3a}$+C$_{3a'}$), 134.42 (C$_{8b'}$), 133.45 (C$_{4a}$ or C$_{4a'}$), 133.42 (C$_{4a}$ or C$_{4a'}$), 129.38 (C$_{4b'}$), 123.38 (C$_{6b}$; C$_{5b}$ or C$_{6b'}$), 123.36 (C$_{6b}$; C$_{5b}$ or C$_{6b'}$), 122.16 (C$_{5b}$ or C$_{6b'}$), 120.81 (C$_{5b'}$), 115.04 (C$_{5a}$ or C$_{9a}$ or C$_{5a'}$ or C$_{9a'}$), 114.92 (C$_{5a}$ or C$_{9a}$ or C$_{5a'}$ or C$_{9a'}$), 113.49 (C$_{5a}$ or C$_{9a}$ or C$_{5a'}$ or C$_{9a'}$), 111.17 (C$_{7b'}$), 69.90 (C$_{10b'}$), 58.35 (C$_{11b'}$) ppm. ^{15}N NMR (50.70 MHz, DMSO-d_6): δ 167.6 (N$_{1a}$+N$_{1a'}$), 121.4 (N$_{1b}$+N$_{1b'}$) ppm.

Synthesis of Organometallic Complexes. *(η^6-p-Cymene){3-(1H-benzimidazol-κN-2-yl)-1H-pyrazolo-κN-[3,4-b]pyridine}chloridoruthenium(II) chloride, [Ru^{II}Cl(η^6-p-cymene)(L1)]Cl, (11a).* A mixture of **L1** (54.7 mg, 0.23 mmol) and [RuCl$_2$(η^6-p-cymene)]$_2$ (70 mg, 0.11 mmol) in dry ethanol (25 mL) was stirred at room temperature for 1 h. Ethanol then was evaporated up to ca. 3 mL and dry Et$_2$O (40 mL) was added. The yellow precipitate was filtered off and dried in vacuo at 50 °C. Yield: 90−95 mg, 70−74% as **11a**·H$_2$O. M_r(C$_{23}$H$_{23}$Cl$_2$N$_5$Ru) = 541.44 g/mol. Anal. Calcd for **11a**·H$_2$O (M_r = 559.45 g/mol): C, 49.38; H, 4.50; N, 12.52; Cl, 12.67. Found: C, 49.68; H, 4.25; N, 12.11; Cl, 12.26. ESI-MS in methanol (positive): m/z 470 [M−HCl−Cl]$^+$, 507 [M−Cl]$^+$, 528 [M−HCl+Na]$^+$; (negative): m/z 468 [M−2HCl−H]$^−$, 505 [M−HCl−H]$^−$. UV−vis (methanol), λ_{max}, nm (ε, M^{-1} cm^{-1}): 251 (16335), 299 (26663), sh 347 (16012). UV−vis (H$_2$O), λ_{max}, nm

(ε, M^{-1} cm^{-1}): sh 245 (10728), 294 (18597), 360 (9666). ^{1}H NMR (500.32 MHz, DMSO-d_6): δ 14.91 (brs, 1H, H$_{1b}$), 9.17 (d, 1H, J = 7.7 Hz, H$_{4a}$), 8.82 (d, 1H, J = 3.8 Hz, H$_{6a}$), 8.11 (d, 1H, J = 7.1 Hz, H$_{4b}$), 7.84 (d, 1H, J = 8.5 Hz, H$_{7b}$), 7.58 (m, 3H, H$_{5a}$+H$_{5b}$+H$_{6b}$), 6.43 (m, 2H, H$_{2c}$+H$_{6c}$), 6.31 (d, 1H, J = 5.3 Hz, H$_{3c}$ or H$_{5c}$), 6.12 (d, 1H, J = 5.5 Hz, H$_{3c}$ or H$_{5c}$), 2.54 (sep, 1H, H$_{7c}$, under DMSO-d_6 peak), 2.21 (s, 3H, H$_{10c}$), 0.94 (d, 3H, J = 6.6 Hz, H$_{8c}$ or H$_{9c}$), 0.91 (d, 3H, J = 6.6 Hz, H$_{8c}$ or H$_{9c}$) ppm. ^{13}C NMR (125.81 MHz, DMSO-d_6): δ 153.97 (C$_{8a}$), 150.45 (C$_{6a}$), 146.52 (C$_{2b}$), 141.37 (C$_{9b}$), 134.70 (C$_{8b}$), 134.64 (C$_{3a}$), 131.48 (C$_{4a}$), 125.39 (C$_{5b}$ or C$_{6b}$), 124.92 (C$_{5b}$ or C$_{6b}$), 119.56 (C$_{5a}$), 117.85 (C$_{4b}$), 113.96 (C$_{7b}$), 111.54 (C$_{9a}$), 103.96 (C$_{4c}$), 103.74 (C$_{1c}$), 84.44 (C$_{2c}$ or C$_{6c}$), 83.73 (C$_{2c}$ or C$_{6c}$), 82.15 (C$_{3c}$ or C$_{5c}$), 80.84 (C$_{3c}$ or C$_{5c}$), 31.12 (C$_{7c}$), 22.19 (C$_{8c}$+C$_{9c}$), 19.17 (C$_{10c}$) ppm. ^{15}N NMR (50.70 MHz, DMSO-d_6): δ 128.7 (N$_{1b}$) ppm.

(η^6-p-Cymene){3-(1H-benzimidazol-κN-2-yl)-1H-pyrazolo-κN-[3,4-b]pyridine}chloridoosmium(II) chloride, [Os^{II}Cl(η^6-p-cymene)-(L1)]Cl, (11b). A mixture of **L1** (42.5 mg, 0.18 mmol) and [OsCl$_2$-(η^6-p-cymene)]$_2$ (70 mg, 0.09 mmol) in dry ethanol (25 mL) was stirred at room temperature for 2 h. Ethanol then was removed under reduced pressure up to ca. 3 mL and dry Et$_2$O (40 mL) was added. The yellow precipitate was filtered off and dried in vacuo at 50 °C. Yield: 93 mg, 81% as **11b**·H$_2$O. M_r(C$_{23}$H$_{23}$Cl$_2$N$_5$Os) = 630.59 g/mol. Anal. Calcd for **11b**·H$_2$O (M_r = 648.61 g/mol): C, 42.59; H, 3.88; N, 10.79. Found: C, 42.56; H, 3.57; N, 10.97. ESI-MS in methanol (positive): m/z [M−HCl−Cl]$^+$, 596 [M−Cl]$^+$, 618 [M−HCl+Na]$^+$; (negative): m/z 595 [M−HCl−H]$^−$. UV−vis (methanol), λ_{max}, nm (ε, M^{-1} cm^{-1}): sh 252 (17048), 299 (20228), 343 (19879). ^{1}H NMR (500.32 MHz, MeOH-d_4): δ 8.99 (dd, 1H, J = 1.3 Hz, J = 8.1 Hz, H$_{4a}$), 8.77 (dd, 1H, J = 1.4 Hz, J = 4.8 Hz, H$_{6a}$), 7.96 (dd, 1H, J = 2.0 Hz, J = 6.4 Hz, H$_{4b}$), 7.80 (dd, 1H, J = 1.9 Hz, J = 6.1 Hz, H$_{7b}$), 7.64−7.59 (m, 3H, H$_{5a}$+H$_{5b}$+H$_{6b}$), 6.66 (d, 1H, J = 5.6 Hz, H$_{2c}$ or H$_{6c}$), 6.59 (d, 1H, J = 5.7 Hz, H$_{2c}$ or H$_{6c}$), 6.43 (d, 1H, J = 5.6 Hz, H$_{3c}$ or H$_{5c}$), 6.21 (d, 1H, J = 5.7 Hz, H$_{3c}$ or H$_{5c}$), 2.43 (sep, 1H, J = 6.9 Hz, H$_{7c}$), 2.38 (s, 3H, H$_{10c}$), 0.96 (d, 3H, J = 6.9 Hz, H$_{8c}$ or H$_{9c}$), 0.92 (d, 3H, J = 6.9 Hz, H$_{8c}$ or H$_{9c}$) ppm. ^{13}C NMR (125.81 MHz, MeOH-d_4): δ 153.25 (C$_{8a}$), 148.91 (C$_{2b}$), 147.42 (C$_{6a}$), 140.49 (C$_{9b}$), 135.15 (C$_{3a}$), 134.25 (C$_{8b}$), 132.07 (C$_{4a}$), 125.47 (C$_{5b}$ or C$_{6b}$), 124.81 (C$_{5b}$ or C$_{6b}$), 118.48 (C$_{5a}$), 116.89 (C$_{4b}$), 112.98 (C$_{7b}$), 112.92 (C$_{9a}$), 97.71 (C$_{4c}$), 94.88 (C$_{1c}$), 76.44 (C$_{2c}$ or C$_{6c}$), 74.99 (C$_{2c}$ or C$_{6c}$), 71.93 (C$_{3c}$ or C$_{5c}$), 70.44 (C$_{2c}$ or C$_{6c}$), 31.37 (C$_{7c}$), 21.35 (C$_{8c}$ or C$_{9c}$), 21.09 (C$_{8c}$ or C$_{9c}$), 17.84 (C$_{10c}$) ppm. Crystals of **11b**·4H$_2$O suitable for XRD study have been obtained from a solution of **11b** in ethanol.

(η^6-p-Cymene){3-(1H-benzimidazol-κN-2-yl)-5-bromo-1H-pyrazolo-κN-[3,4-b]pyridine}chloridoruthenium(II) chloride, [Ru^{II}Cl(η^6-p-cymene)(L2)]Cl, (12a). A mixture of **L2** (73.2 mg, 0.23 mmol) and [RuCl$_2$(η^6-p-cymene)]$_2$ (70 mg, 0.11 mmol) in dry ethanol (25 mL) was stirred at room temperature for 1 h. Ethanol then was removed under reduced pressure up to ca. 2 mL and dry Et$_2$O (40 mL) was added. The yellow precipitate was filtered off and dried in vacuo at 40 °C. Yield: 106 mg, 73% as **12a**·H$_2$O. M_r(C$_{23}$H$_{22}$BrCl$_2$N$_5$Ru) = 620.33 g/mol. Anal. Calcd for **12a**·H$_2$O (M_r = 638.35 g/mol): C, 43.28; H, 3.79; N, 10.97. Found: C, 43.42; H, 3.54; N, 11.18. ESI-MS in methanol (positive): m/z 548 [M−HCl−Cl]$^+$, 608 [M−HCl+Na]$^+$; (negative): m/z 549 [M−2HCl−H]$^−$, 582 [M−HCl−H]$^−$. UV−vis (methanol), λ_{max}, nm (ε, M^{-1} cm^{-1}): sh 254 (17778), 303 (29953), 351 (17387). ^{1}H NMR (500.32 MHz, DMSO-d_6): δ 14.34 (brs, 1H, H$_{1b}$), 9.21 (s, 1H, H$_{4a}$), 8.73 (s, 1H, H$_{6a}$), 8.06 (d, 1H, J = 7.6 Hz, H$_{4b}$), 7.79 (d, 1H, J = 8.5 Hz, H$_{7b}$), 7.52 (m, 2H, H$_{5b}$+H$_{6b}$), 6.32 (d, 2H, J = 5.8 Hz, H$_{2c}$+H$_{6c}$), 6.22 (d, 1H, J = 6.2 Hz, H$_{3c}$ or H$_{5c}$), 6.03 (d, 1H, J = 6.1 Hz, H$_{3c}$ or H$_{5c}$), 2.52 (sep, 1H, H$_{7c}$, under DMSO-d_6 peak), 2.18 (s, 3H, H$_{10c}$), 0.94 (d, 3H, J = 6.8 Hz, H$_{8c}$ or H$_{9c}$), 0.89 (d, 3H, J = 6.9 Hz, H$_{8c}$ or H$_{9c}$) ppm. ^{13}C NMR (125.81 MHz, DMSO-d_6): δ 154.04 (C$_{8a}$), 151.24 (C$_{6a}$), 146.57 (C$_{2b}$), 141.37 (C$_{9b}$), 134.63 (C$_{8b}$), 133.43 (C$_{3a}$), 131.82 (C$_{4a}$), 125.33 (C$_{5b}$ or C$_{6b}$), 124.88 (C$_{5b}$ or C$_{6b}$), 117.78 (C$_{4b}$), 114.72 (C$_{5a}$ or C$_{9a}$),

113.85 (C_{7b}), 112.48 (C_{5a} or C_{9a}), 103.96 (C_{4c}), 103.74 (C_{1c}), 84.44 (C_{2c} or C_{6c}), 83.69 (C_{2c} or C_{6c}), 82.16 (C_{3c} or C_{5c}), 80.76 (C_{3c} or C_{5c}), 31.09 (C_{7c}), 22.20 (C_{8c} or C_{9c}), 22.17 (C_{8c} or C_{9c}), 19.16 (C_{10c}) ppm. ^{15}N NMR (50.70 MHz, DMSO-d_6): δ 127.3 (N_{1b}) ppm.

(η^6-p-Cymene){3-(1H-benzimidazol-κN-2-yl)-5-bromo-1H-pyrazolo-κN-[3,4-b]pyridine}chloridoosmium(II) chloride, [$Os^{II}Cl(\eta^6$-p-cymene)-(**L2**)]Cl, (**12b**). A mixture of **L2** (56.4 mg, 0.18 mmol) and [$OsCl_2(\eta^6$-p-cymene)]$_2$ (70 mg, 0.09 mmol) in dry ethanol (25 mL) was stirred at room temperature for 2 h. Ethanol then was removed under reduced pressure up to ca. 3 mL and dry Et_2O (40 mL) was added. The yellow precipitate was filtered off and dried in vacuo at 50 °C. Yield: 102 mg, 79% as **12b**·H_2O. M_r($C_{23}H_{22}BrCl_2N_5Os$) = 709.49 g/mol. Anal. Calcd for **12b**·H_2O (M_r = 727.51 g/mol): C, 37.97; H, 3.33; N, 9.63. Found: C, 37.82; H, 3.02; N, 9.33. ESI-MS in methanol (positive): m/z 638 [M−HCl−Cl]$^+$, 696 [M−HCl+Na]$^+$; (negative): m/z 672 [M−HCl−H]$^-$. UV−vis (methanol), λ_{max}, nm (ε, M^{-1} cm^{-1}): sh 253 (21638), 302 (30505), 357 (21813). ^{1}H NMR (500.32 MHz, MeOH-d_4): δ 9.08 (d, 1H, J = 2.1 Hz, H_{4a}), 8.84 (d, 1H, J = 2.1 Hz, H_{6a}), 7.96 (dd, 1H, J = 2.1 Hz, J = 6 Hz, H_{4b}), 7.80 (dd, 1H, J = 2.1 Hz, J = 6.1 Hz, H_{7b}), 7.63 (m, 2H, H_{5b}+H_{6b}), 6.69 (d, 1H, J = 5.7 Hz, H_{2c} or H_{6c}), 6.63 (d, 1H, J = 5.6 Hz, H_{2c} or H_{6c}), 6.48 (d, 1H, J = 5.6 Hz, H_{3c} or H_{5c}), 6.22 (d, 1H, J = 5.7 Hz, H_{3c} or H_{5c}), 2.42 (sep, 1H, J = 6.9 Hz, H_{7c}), 2.39 (s, 3H, H_{10c}), 0.95 (d, 3H, J = 6.9 Hz, H_{8c} or H_{9c}), 0.91 (d, 3H, J = 6.9 Hz, H_{8c} or H_{9c}) ppm. ^{13}C NMR (125.81 MHz, MeOH-d_4): δ 153.04 (C_{8a}), 152.49 (C_{6a}), 148.15 (C_{2b}), 140.47 (C_{9b}), 134.58 (C_{3a}), 134.19 (C_{8b}), 131.13 (C_{4a}), 125.79 (C_{5b} or C_{6b}), 125.05 (C_{5b} or C_{6b}), 116.99 (C_{4b}), 115.39 (C_{5a} or C_{9a}), 113.09 (C_{7b}), 112.11 (C_{5a} or C_{9a}), 98.54 (C_{4c}), 95.52 (C_{1c}), 75.73 (C_{2c} or C_{6c}), 75.25 (C_{2c} or C_{6c}), 71.87 (C_{3c} or C_{5c}), 69.99 (C_{3c} or C_{5c}), 31.41 (C_{7c}), 21.34 (C_{8c} or C_{9c}), 21.16 (C_{8c} or C_{9c}), 17.84 (C_{10c}) ppm. Crystals of **12b** and **12b**·2CH_3OH·2H_2O suitable for XRD study have been obtained from a solution of **12b** in methanol.

(η^6-p-Cymene){5-bromo-3-(7-methoxymethyl-1H-benzimidazol-κN-2-yl)-1H-pyrazolo-κN-[3,4-b]pyridine}chloridoruthenium(II) chloride, [$Ru^{II}Cl(\eta^6$-p-cymene)(**L3**)]Cl, (**13a**). A mixture of **L3** (64 mg, 0.18 mmol) and [$RuCl_2(\eta^6$-p-cymene)]$_2$ (50 mg, 0.08 mmol) in dry ethanol (25 mL) was stirred at room temperature for 1 h. Ethanol then was removed under reduced pressure up to ca. 3 mL and dry Et_2O (40 mL) was added. The yellow precipitate was filtered off and dried in vacuo at 50 °C. Yield: 95.8 mg, 85% as **13a**·1.5H_2O. M_r($C_{25}H_{26}BrCl_2N_5ORu$) = 664.39 g/mol. Anal. Calcd for **13a**·1.5H_2O (M_r = 691.41 g/mol): C, 43.43; H, 4.23; N, 10.13; Cl, 10.26. Found: C, 43.81; H, 4.24; N, 10.11; Cl, 10.57. ESI-MS in methanol (positive): m/z 592 [M−HCl−Cl]$^+$, 650 [M−HCl+Na]$^+$; (negative): m/z 591 [M−2HCl−H]$^-$, 628 [M−HCl−H]$^-$. UV−vis (methanol), λ_{max}, nm (ε, M^{-1}cm^{-1}): sh 252 (18744), 306 (28529), 354 (16889). ^{1}H NMR (500.32 MHz, DMSO-d_6): δ 13.88 (brs, 1H, H_{1b}), 9.41 (s, 1H, H_{4a}), 8.68 (s, 1H, H_{6a}), 7.99 (d, 1H, J = 7.7 Hz, H_{4b}), 7.49 (m, 2H, H_{5b}+H_{6b}), 6.29 (m, 2H, H_{2c}+H_{6c}), 6.20 (d, 1H, J = 5.5 Hz, H_{3c} or H_{5c}), 6.00 (d, 1H, J = 5.9 Hz, H_{3c} or H_{5c}), 4.88 (s, 2H, H_{10b}), 3.39 (s, 3H, H_{11b}), 2.48 (sep, 1H, H_{7c}, under DMSO-d_6 peak), 2.17 (s, 3H, H_{10c}), 0.93 (d, 3H, J = 6.9 Hz, H_{8c} or H_{9c}), 0.87 (d, 3H, J = 6.8 Hz, H_{8c} or H_{9c}) ppm. ^{13}C NMR (125.81 MHz, DMSO-d_6): δ 155.35 (C_{8a}), 150.27 (C_{6a}), 147.43 (C_{2b}), 141.64 (C_{9b}), 133.07 (C_{8b}), 132.68 (C_{3a}), 131.68 (C_{4a}), 124.87 (C_{5b} or C_{6b}), 124.59 (C_{5b} or C_{6b}), 124.53 (C_{7b}), 117.18 (C_{4b}), 114.23 (C_{5a} or C_{9a}), 112.78 (C_{5a} or C_{9a}), 103.74 (C_{4c}), 103.09 (C_{1c}), 85.38 (C_{2c} or C_{6c}), 83.68 (C_{2c} or C_{6c}), 82.13 (C_{3c} or C_{5c}), 81.05 (C_{3c} or C_{5c}), 70.19 (C_{10b}), 58.03 (C_{11b}), 31.04 (C_{7c}), 22.22 (C_{8c} or C_{9c}), 22.09 (C_{8c} or C_{9c}), 19.13 (C_{10c}) ppm. ^{15}N NMR (50.70 MHz, DMSO-d_6): δ 122.9 (N_{1b}) ppm. The red XRD-quality crystals of [$Ru^{II}Cl(\eta^6$-p-cymene)(**L3**−H)] (**13c**) were obtained from EtOH/Et_2O and an EtOH solution of **13a** (long crystallization). The yellow crystals of [$Ru^{II}Cl(\eta^6$-p-cymene)(**L3**)]Cl·[$Ru^{II}Cl(\eta^6$-p-cymene)(**L3**−H)]·CH_3OH (**13d**·CH_3OH) suitable for XRD study have been obtained from methanolic solution of **13a** (short crystallization). ^{1}H NMR (**13c**, 500.32 MHz, DMSO-d_6): δ 13.43 (s, 1H),

9.18 (d, 1H, J = 2.1 Hz), 8.48 (d, 1H, J = 2.2 Hz), 7.94 (d, 1H, J = 8.2 Hz), 7.45 (t, 1H, J = 7.8 Hz), 7.39 (d, 1H, J = 7.2 Hz), 6.16 (d, 1H, J = 6.0 Hz), 6.13 (d, 1H, J = 6.1 Hz), 6.07 (d, 1H, J = 5.9 Hz), 5.89 (d, 1H, J = 6.4 Hz), 4.85 (s, 2H), 4.04 (s, 3H), 2.14 (s, 3H), 0.93 (d, 3H, J = 6.8 Hz), 0.86 (d, 3H, J = 6.9 Hz) ppm.

(η^6-p-Cymene){5-bromo-3-(7-methoxymethyl-1H-benzimidazol-κN-2-yl)-1H-pyrazolo-κN-[3,4-b]pyridine}chloridoosmium(II) chloride, [$Os^{II}Cl(\eta^6$-p-cymene)(**L3**)]Cl, (**13b**). A mixture of **L3** (59 mg, 0.17 mmol) and [$OsCl_2(\eta^6$-p-cymene)]$_2$ (60 mg, 0.08 mmol) in dry ethanol (25 mL) was stirred at room temperature for 3 h. Ethanol was evaporated up to ca. 3 mL and dry Et_2O (40 mL) was added. The yellow precipitate was filtered off and dried in vacuo at 50 °C. Yield: 80 mg, 70%. M_r($C_{25}H_{26}BrCl_2N_5OOs$) = 753.55 g/mol. Anal. Calcd for **13b**: C, 39.85; H, 3.48; N, 9.29. Found: C, 39.60; H, 3.32; N, 9.20. ESI-MS in methanol (positive): m/z 682 [M−HCl−Cl]$^+$, 704 [M−2HCl+Na]$^+$; (negative): m/z 680 [M−2HCl−H]$^-$, 716 [M−HCl−H]$^-$. UV−vis (methanol), λ_{max}, nm (ε, M^{-1} cm^{-1}): sh 256 (19825), 303 (24634), 357 (18850). ^{1}H NMR (500.32 MHz, MeOH-d_4): δ 9.33 (d, 1H, J = 2.1 Hz, H_{4a}), 8.84 (d, 1H, J = 2.2 Hz, H_{6a}), 7.91 (dd, 1H, J = 1.2 Hz, J = 7.8 Hz, H_{4b}), 7.64−7.58 (m, 2H, H_{5b}+H_{6b}), 6.69 (d, 1H, J = 5.6 Hz, H_{2c} or H_{6c}), 6.62 (d, 1H, J = 5.7 Hz, H_{2c} or H_{6c}), 6.47 (d, 1H, J = 5.5 Hz, H_{3c} or H_{5c}), 6.21 (d, 1H, J = 5.6 Hz, H_{3c} or H_{5c}), 4.94 (q, 2H, J = 12.4 Hz, H_{10b}), 3.49 (s, 3H, H_{11b}), 2.41 (sep, 1H, J = 6.9 Hz, H_{7c}), 2.39 (s, 3H, H_{10c}), 0.94 (d, 3H, J = 6.9 Hz, H_{8c} or H_{9c}), 0.89 (d, 3H, J = 6.9 Hz, H_{8c} or H_{9c}) ppm. ^{13}C NMR (125.81 MHz, MeOH-d_4): δ 153.18 (C_{8a}), 152.16 (C_{6a}), 148.36 (C_{2b}), 140.82 (C_{9b}), 134.35 (C_{3a}), 132.68 (C_{8b}), 131.68 (C_{4a}), 125.63 (C_{5b} or C_{6b}), 124.85 (C_{5b} or C_{6b}), 124.51 (C_{7b}), 116.72 (C_{4b}), 115.24 (C_{5a} or C_{9a}), 112.26 (C_{5a} or C_{9a}), 98.75 (C_{4c}), 95.50 (C_{1c}), 75.98 (C_{2c} or C_{6c}), 75.34 (C_{2c} or C_{6c}), 71.82 (C_{3c} or C_{5c}), 70.29 (C_{10b}), 70.04 (C_{3c} or C_{5c}), 57.17 (C_{11b}), 31.39 (C_{7c}), 21.34 (C_{8c} or C_{9c}), 21.16 (C_{8c} or C_{9c}), 17.85 (C_{10c}) ppm. The yellow crystals of [$Os^{II}Cl(\eta^6$-p-cymene)(**L3**)]Cl·[$Os^{II}Cl(\eta^6$-p-cymene)(**L3**−H)]·0.75 CH_3OH·0.25H_2O (**13e**·0.75CH_3OH·0.25H_2O) suitable for XRD study have been obtained from a methanolic solution of **13b**.

Physical Measurements. Elemental analyses (C, H, N, Cl) were performed by the Microanalytical Service of the Institute of Physical Chemistry, University of Vienna. Electrospray ionization mass spectrometry (ESI-MS) was carried out with an Esquire 3000 instrument (Bruker Daltonics, Bremen, Germany), using solutions of compounds in methanol. The expected and measured isotope distributions were compared. UV−vis spectra were recorded on a Lambda 20 UV−vis spectrophotometer (Perkin−Elmer), using samples dissolved in methanol (**L1**−**L3**, **11a**, **12a**, **13a**, **11b**, **12b**, **13b**) and water (**11a**) over 24 or 48 h, correspondingly. The one-dimensional (^{1}H, ^{13}C, ^{15}N) and two-dimensional spectra (^{15}N,^{1}H HSQC, ^{13}C,^{1}H HSQC, ^{13}C,^{1}H HMBC, ^{1}H,^{1}H COSY, ^{1}H,^{1}H TOCSY, ^{1}H,^{1}H NOESY (**L3**, **12a**), ^{1}H,^{1}H ROESY (**L3**, **11a**, **12a**, **13a**, **13b**)) were recorded with a Bruker Model DPX500 (Ultrashield Magnet) system in DMSO-d_6 (**L1**−**L3**, **11a**, **12a**, **13a**), MeOH-d_4 (**11b**, **12b**, **13b**), D_2O (^{1}H NMR, **11a**), and D_2O/DMSO-d_6 (^{1}H NMR, **12a**), using standard pulse programs at 500.32 (^{1}H), 125.81 (^{13}C) and 50.70 (^{15}N) MHz. ^{1}H signals are referenced relative to the solvent signals (DMSO-d_6 at 2.51, MeOH-d_4 at 3.33 ppm).

Crystallographic Structure Determination. XRD measurements were performed on a Bruker Model X8 APEXII CCD diffractometer. Single crystals were positioned at distances of 35, 40, 40, 40, 40, 40, and 35 mm from the detector, and 1556, 1131, 518, 1911, 1176, 1978, and 1039 frames were measured, each for 30, 60, 30, 20, 70, 60, and 30 s over 1° scan width for **2**·0.5H_2O, **11b**·4H_2O, **12b**, **12b**·2CH_3OH· 2H_2O, **13c**, **13d**·CH_3OH, and **13e**·0.75CH_3OH·0.25H_2O, correspondingly. The data were processed using SAINT software.[39] Crystal data, data collection parameters, and structure refinement details are given in Table 1. The structures were solved by direct methods and refined by full-matrix least-squares techniques. Non-H atoms were

11719

dx.doi.org/10.1021/ic201704u |*Inorg. Chem.* 2011, 50, 11715–11728

Table 1. Crystal Data and Details of Data Collection for 2·0.5H$_2$O, 11b·4H$_2$O, 12b, 12b·2CH$_3$OH·2H$_2$O, 13c, 13d·CH$_3$OH, and 13e·0.75CH$_3$OH·0.25H$_2$O

	2·0.5H$_2$O	11b·4H$_2$O	12b	12b·2CH$_3$OH·2H$_2$O	13c	13d·CH$_3$OH	13e·0.75CH$_3$OH·0.25H$_2$O
empirical formula	C$_7$H$_7$BrN$_3$O$_{0.5}$	C$_{23}$H$_{31}$Cl$_2$N$_5$O$_4$Os	C$_{23}$H$_{22}$BrCl$_2$N$_5$Os	C$_{25}$H$_{34}$BrCl$_2$N$_5$O$_4$Os	C$_{25}$H$_{35}$BrClN$_5$ORu	C$_{51}$H$_{55}$Br$_2$Cl$_3$N$_{10}$O$_3$Ru$_2$	C$_{50.75}$H$_{54.5}$Br$_2$Cl$_3$N$_{10}$O$_3$Os$_2$
formula wt, Fw	221.06	702.63	709.47	809.58	627.93	1324.36	1499.11
space group	P1̄	P2$_1$/c	P2$_1$/n	P1̄	P2$_1$/c	P1̄	P1̄
a [Å]	7.0878(3)	19.2075(13)	8.5092(10)	8.4014(8)	16.7948(13)	9.9942(9)	10.0042(5)
b [Å]	7.5561(3)	7.7890(5)	19.402(3)	13.1678(14)	12.4936(10)	15.4370(13)	15.3936(8)
c [Å]	16.5281(8)	17.0807(11)	14.497(3)	13.7997(16)	12.3028(8)	17.8076(17)	17.8050(9)
α [°]	98.267(3)			81.446(4)		104.380(5)	104.233(2)
β [°]	97.046(3)	99.334(4)	91.531(5)	81.191(5)	108.744(5)	93.139(5)	93.029(2)
γ [°]	107.894(3)			76.887(5)		98.859(4)	98.683(3)
V [Å^3]	820.42(6)	2521.6(3)	2392.5(6)	1458.9(3)	2444.6(3)	2617.1(4)	2615.7(2)
Z	4	4	4	2	4	2	2
λ [Å]	0.71073	0.71073	0.71073	0.71073	0.71073	0.71073	0.71073
ρ$_{calcd}$ [g cm^{-3}]	1.790	1.851	1.970	1.843	1.706	1.681	1.903
crystal size [mm^3]	0.20 × 0.15 × 0.05	0.20 × 0.10 × 0.02	0.20 × 0.04 × 0.04	0.20 × 0.04 × 0.04	0.20 × 0.05 × 0.02	0.20 × 0.20 × 0.20	0.25 × 0.17 × 0.05
temp, T [K]	120(2)	100(2)	100(2)	100(2)	296(2)	100(2)	100(2)
μ [mm^{-1}]	4.954	5.309	7.245	5.962	2.414	2.310	6.587
R$_1$[a]	0.0434	0.0531	0.0560	0.0310	0.0547	0.0512	0.0442
wR$_2$[b]	0.1181	0.1072	0.1221	0.0796	0.1355	0.1411	0.1055
goodness of fit, GOF[c]	1.092	1.011	0.939	1.087	0.986	1.048	1.054

[a] $R_1 = \Sigma||F_o| - |F_c||/\Sigma|F_o|$. [b] $wR_2 = \{\Sigma[w(F_o^2 - F_c^2)^2]/\Sigma[w(F_o^2)^2]\}^{1/2}$. [c] GOF $= \{\Sigma[w(F_o^2 - F_c^2)^2]/(n - p)\}^{1/2}$, where n is the number of reflections and p is the total number of parameters refined.

refined with anisotropic displacement parameters. H atoms were inserted in calculated positions and refined with a riding model. Refinement of the structure of **12b** revealed that the chloride counteranion occupies two statistically disordered positions with site occupation factor (sof) values of 0.57:0.43, whereas, in **13c**, the methoxymethylene group was found to be disordered over two positions with sof values of 0.80:0.20. Similarly, the methoxymethylene group of one crystallographically independent complex in **13d·CH$_3$OH** or in both crystallographically independent complexes in **13e·0.75CH$_3$OH·0.25H$_2$O** is disordered with sof values of 0.35:0.65 and 0.60:0.40, 0.80:0.20, correspondingly. The disorder was resolved with constrained anisotropic displacement parameters and restrained bond distances using EADP and SADI instructions of SHELX97, respectively. Structure solution was achieved with SHELXS-97 and refinement with SHELXL-97,[40] and graphics were produced with ORTEP-3.[41]

Cell Lines and Culture Conditions. A549 (non-small cell lung carcinoma, human) and SW480 (colon carcinoma, human) cells were kindly provided by Brigitte Marian (Institute of Cancer Research, Department of Medicine I, Medical University of Vienna, Austria). CH1 cells (ovarian cancer, human) were a gift from Lloyd R. Kelland (CRC Centre for Cancer Therapeutics, Institute of Cancer Research, Sutton, U.K.). All cell culture media and supplements were purchased from Sigma—Aldrich. Cells were grown in 75-cm^2 culture flasks (Iwaki) in a complete medium (i.e., Minimum Essential Medium supplemented with 10% heat-inactivated fetal bovine serum, 1 mM sodium pyruvate, 4 mM L-glutamine, and 1% nonessential amino acids from 100× stock) as adherent monolayer cultures. Cultures were grown at 37 °C under a humidified atmosphere containing 5% CO$_2$ and 95% air.

Inhibition of Cancer Cell Growth. Antiproliferative activity in vitro was determined by the colorimetric MTT assay (MTT = 3-(4,5-dimethyl-2-thiazolyl)-2,5-diphenyl-2H-tetrazolium bromide, Fluka). For this purpose, cells were harvested from culture flasks by the use of trypsin and seeded in complete medium (100 μL/well) into 96-well plates (Iwaki) in densities of 4 × 10^3 (A549), 1.5 × 10^3 (CH1), and 2.5 × 10^3 (SW480) viable cells per well. Cells were allowed for 24 h to settle and resume proliferation. Test compounds were dissolved in DMSO first, appropriately diluted in complete medium, and instantly added to the plates (100 μL/well), where the DMSO content did not exceed 0.4% and 1% for the ligands and complexes, respectively. After exposure for 96 h, the medium was replaced with 100 μL/well RPMI 1640 medium (supplemented with 10% heat-inactivated fetal bovine serum and 4 mM L-glutamine) plus 20 μL/well MTT solution in phosphate-buffered saline (5 mg/mL), followed by incubation for 4 h. Subsequently, the medium/MTT mixture was removed, and the formazan product formed by viable cells was dissolved in DMSO (150 μL/well). Optical densities were measured with a microplate reader (Tecan Spectra Classic) at 550 nm (and a reference wavelength of 690 nm) to yield relative quantities of viable cells as percentages of untreated controls, and 50% inhibitory concentrations (IC$_{50}$) were interpolated from concentration—effect curves. Calculations are based on at least three independent experiments with triplicates for each concentration level.

Cell Cycle Analyses. To study the effects on the cell cycle of exponentially growing CH1 cells by flow cytometric analysis of their relative DNA content, cells were harvested from culture flasks, seeded in complete medium into 90-mm Petri dishes (1 × 10^6 cells/dish) and, after recovery for 24 h, exposed to various concentrations of the test compounds for 24 h. For this purpose, test compounds were diluted from DMSO stocks with complete medium (see above) such that the effective DMSO content did not exceed 0.5%. After exposure, treated and control cells were collected by scratching, washed with PBS, and stained with 5 μg/mL propidium iodide overnight. Their fluorescence was measured with a FACS Calibur instrument (Becton Dickinson), and the obtained histograms were analyzed with Cell Quest Pro software (Becton Dickinson).

Scheme 1. Synthesis of 5-Bromo-1*H*-pyrazolo[3,4-*b*]-pyridine-3-carboxylic acid (3)[a]
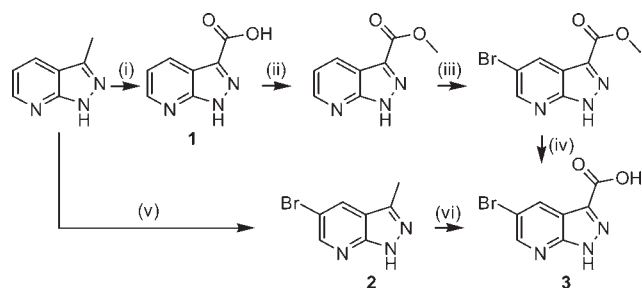
[a] Reagents and conditions: (i) KMnO₄, NaOH, 3 h, 100 °C, H₂SO₄;[35] (ii) methanol, H₂SO₄, reflux, 6−8 h, NaHCO₃, 42% (i + ii);[35] (iii) Br₂, AcOH, AcONa, 115 °C, overnight, chromatographic purification, 43%;[23] (iv) NaOH, MeOH, reflux, 4 h, HCl, 100%;[23] (v) Br₂, AcOH, AcONa, 115 °C, 2.5−3 h; and (vi) KMnO₄, NaOH, 3 h, 100 °C, HCl, 24−35% (v + vi).

At least two independent experiments were performed for each setting, and 2.5 or 3.0 × 10⁴ cells were measured per sample.

Kinase Assay. The Cdk-inhibitory capacities of test compounds were studied by a radiochemical assay using recombinant Cdk1/cyclin B and Cdk2/cyclin E isolated from Sf21 insect cells and histone H1 as the substrate for phosphorylation, as described by Marko et al.[42] Briefly, MOPS-buffered assay mixtures containing the test compound (with a maximum of 1% DMSO), the respective kinase/cyclin complex, histone H1, and 0.4 μCi (γ-³²P)ATP per sample were incubated for 10 min at 30 °C. Aliquots of the solution were spotted onto phosphocellulose squares, which had been washed three times with 0.75% phosphoric acid, followed by acetone. The dried squares were measured in scintillation vials by β-counting (Perkin−Elmer Tri-Carb 2800TR; Quanta Smart software). Results were obtained in duplicate in at least two independent experiments, and IC₅₀ values were calculated by interpolation.

■ RESULTS AND DISCUSSION

Synthesis of Ligands and Complexes. Several routes to 3-(1*H*-benzimidazol-2-yl)-1*H*-pyrazolo[3,4-*b*]pyridines have been proposed by Johnson & Johnson Pharmaceutical Research & Development L.L.C. The first one was developed for 3-(1*H*-benzimidazol-2-yl)-1*H*-pyrazolo[3,4-*b*]pyridines with an un-substituted benzimidazole moiety and involved sulfur-induced benzimidazole ring formation via the treatment of 5-bromo-1*H*-pyrazolo[3,4-*b*]pyridine-3-carboxaldehyde with 1,2-diamino-benzene.[22] The poor reproducibility of this synthesis prompted the exploration of an alternative way, via 5-bromo-1*H*-pyrazolo[3,4-b]pyridine-3-carboxylic acid, which was used for the preparation of 3-(1*H*-benzimidazol-2-yl)-1*H*-pyrazolo[3,4-*b*]pyridines with a sub-stituted benzimidazole moiety.

The patented route to 5-bromo-1*H*-pyrazolo[3,4-*b*]pyridine-3-carboxylic acid (3) consists of four steps (see Scheme 1, steps i−iv): oxidation of 3-methyl-1*H*-pyrazolo[3,4-*b*]pyridine by KMnO₄ in the presence of a base with subsequent acidification with H₂SO₄,[35] esterification of 1*H*-pyrazolo[3,4-*b*]pyridine-3-car-boxylic acid (1) in the presence of H₂SO₄ in methanol,[35] bromination of 1*H*-pyrazolo[3,4-*b*]pyridine-3-carboxylic acid methyl ester in an AcOH/AcONa mixture,[23] and hydrolysis of 5-bromo-1*H*-pyrazolo[3,4-*b*]pyridine-3-carboxylic acid methyl es-ter in the presence of NaOH, followed by acidification with HCl.[23]

Scheme 2. Synthesis of 1-Methoxymethyl-2,3-diamino-benzene (5)[a]
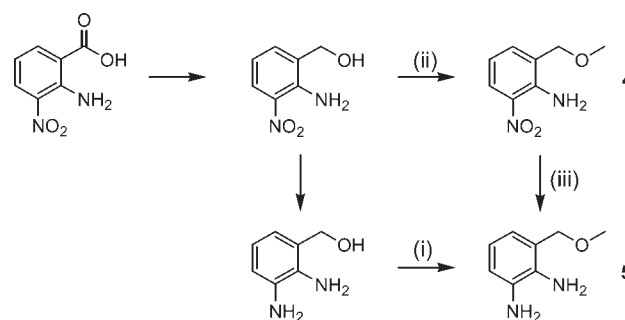
[a] Reagents and conditions: (i) NaH, MeI, dry THF, 0 °C, 30 min, room temperature, overnight, chromatographic purification, 34% yield;[23] (ii) NaH, MeI, dry THF, 0 °C, 15 min, room temperature, 3 h, chromato-graphic purification, 65−75% yield; (iii) 10% Pd/C, ethanol, H₂, room temperature, 18−24 h, 100% yield.

The overall yield of 5-bromo-1*H*-pyrazolo[3,4-*b*]pyridine-3-car-boxylic acid (3) was 18%.

We performed the synthesis of 3 in two steps (see Scheme 1, steps v and vi): bromination of 3-methyl-1*H*-pyrazolo[3,4-*b*]-pyridine in AcOH/AcONa mixture and oxidation of crude 5-bromo-3-methyl-1*H*-pyrazolo[3,4-*b*]pyridine (2) by KMnO₄ in a basic medium, followed by acidification with 37% HCl, with an overall yield of 24−35%. 5-Bromo-3-methyl-1*H*-pyrazolo-[3,4-*b*]pyridine (2) is a known compound, the synthesis of which is well-documented.[43−45]

For the benzimidazole ring formation, 1,2-diaminobenzene and 1-methoxymethyl-2,3-diaminobenzene have been used. The reported synthesis of 1-methoxymethyl-2,3-diaminobenzene (5) from 2,3-diaminobenzyl alcohol afforded the desired product in 34% yield (see Scheme 2, step i).[23] However, the instability and low yield of diamines, as well as the necessity to purify the desired ether using column chromatography, stimulated the search for a more-convenient procedure that was subsequently proposed: etherification of 2-amino-3-nitrobenzyl alcohol, followed by the reduction of 1-methoxymethyl-2-amino-3-nitrobenzene (4) with 10% Pd/C in ethanol under a hydrogen atmosphere afforded 5 in 65−75% yield (see Scheme 2, steps ii and iii).

Patented benzimidazole ring formation by cyclization of the 3-carboxyl group of 5-bromo-1*H*-pyrazolo[3,4-*b*]pyridine-3-car-boxylic acid (3) with substituted 1,2-diaminobenzenes was realized via amide formation using coupling reagents, followed by treatment with glacial acetic acid.[21] HATU (*N*,*N*,*N'*,*N'*-tetramethyl-*O*-(7-azabenzotriazol-1-yl)uronium hexafluoro-phosphate) was used as a coupling reagent.[21,23]

Three 3-(1*H*-benzimidazol-2-yl)-1*H*-pyrazolo[3,4-*b*]pyridines (**L1**−**L3**) (where X = H, Br; and Y = H, CH₂OCH₃) have been synthesized in this work (see Chart 1): *3-(1H-benzimidazol-2-yl)-1H-pyrazolo[3,4-b]pyridine* (**L1**) is a new compound that we have prepared as a model ligand for coordination to metals; *3-(1H-benzimidazol-2-yl)-5-bromo-1H-pyrazolo[3,4-b]pyridine* (**L2**) was previously known as *BOC*-protected compound prepared *via* 5-bromo-1*H*-pyrazolo[3,4-*b*]pyridine-3-carboxaldehyde;[23] *5-bro-mo-3-(4-methoxymethyl-1H-benzimidazol-2-yl)-1H-pyrazolo[3,4-b]-pyridine* (**L3**) was synthesized via 5-bromo-1*H*-pyrazolo[3,4-*b*]-pyridine-3-carboxylic acid (3) and patented as a potential Cdk inhibitor and antiproliferative agent.[23]

Scheme 3. Synthesis of 3-(1H-Benzimidazol-2-yl)-1H-pyrazolo[3,4-b]pyridines L1−L3[a]

X = H (**1**)
X = Br (**3**)

X = H (**6**)
X = Br (**7**)

X = H, Y = H (**8**)
X = Br, Y = H (**9**)
X = Br, Y = CH$_2$OCH$_3$ (**10**)

X = H, Y = H (**L1, 11**)
X = Br, Y = H (**L2, 12**)
X = Br, Y = CH$_2$OCH$_3$ (**L3, 13**)

[a] Reagents and conditions: (i) CDI, dry DMF, room temperature, 20−24 h; (ii) 1,2-diaminobenzene or **5**, dry DMF, 80−85 °C; 5−20 h; and (iii) glacial AcOH, 120−125 °C, 2.5−4.5 h, chromatographic purification.

Figure 1. Part of the ^{1}H,^{1}H ROESY plot of **L3**.

For the synthesis of **L1**−**L3**, we used N,N′-carbonyldiimidazole (CDI) as an amide-coupling reagent, because it is relatively inexpensive and the side products, carbon dioxide and imidazole, could be easily removed from the reaction mixture.

CDI-mediated amidation of acids **1** and **3** was performed as shown in Scheme 3 (steps i and ii). In the first step, the acyl-imidazolides **6** and **7** were obtained in dry DMF at room temperature and isolated as white solids. The yields based on 3-methyl-1H-pyrazolo[3,4-b]pyridine are: 25−29% (**6**) and 13−16% (**7**). In the second step, monoacylation of phenylene-diamines (1,2-diaminobenzene and 1-methoxymethyl-2,3-diami-nobenzene (**5**)) using acyl-imidazolides was performed in DMF at 80−85 °C.

Amides **8**−**10** were used without further purification in ring closure reactions in a glacial acetic acid at 120−125 °C and afforded the desired 3-(1H-benzimidazol-2-yl)-1H-pyrazolo[3,4-b]-pyridines: **L1** (55−60%), **L2** (58−61%), and **L3** (44−51%), based on **6** and **7** (see Scheme 3, step iii). The reported synthesis of **L3** is a one-pot approach for amide formation using HATU with 57% yield, followed by cyclization under acidic conditions (acetic acid) with 87% yield.

Thus, the ligands **L1**, **L2**, and **L3** have been prepared in 7, 8, and 11 steps, correspondingly.

Finally, the ligands **L1**−**L3** were reacted with [M^{II}Cl$_2$(η^6-p-cymene)]$_2$ (where M = Ru, Os) in a 2:1 molar ratio in dry ethanol at room temperature to give [MCl(η^6-arene)(L)]Cl complexes

(**11a**, **11b**, **12a**, **12b**, **13a**, **13b**) in quantitative yields. Crystal-lization of [Ru^{II}Cl(η^6-p-cymene)(L3)]Cl (**13a**) in EtOH or EtOH/Et$_2$O resulted in XRD-quality crystals of [Ru^{II}Cl(η^6-p-cymene)(L3−H)] (**13c**), while the crystallization of **13a** in methanol afforded crystals of composition [Ru^{II}Cl(η^6-p-cymene)(L3)]Cl· [Ru^{II}Cl(η^6-p-cymene)(L3−H)]·CH$_3$OH (**13d**·CH$_3$OH). The osmium(II) analogue **13e**·0.75CH$_3$OH·0.25H$_2$O was obtained via the crystallization of **13b** in methanol.

NMR Evidence of Ligand Coordination. The full assignment of proton, carbon, and nitrogen resonances for **L1**−**L3**, **11a**, **11b**, **12a**, **12b**, **13a**, and **13b** is quoted in Tables S1−S3 in the Supporting Information.

3-(1H-Benzimidazol-2-yl)-1H-pyrazolo[3,4-b]pyridines with an unsubstituted benzimidazole moiety (**L1**, **L2**) display one set of signals. **L1** is characterized by three doublets of doublets for H$_{4a}$, H$_{5a}$, H$_{6a}$ (8.85, 7.39, 8.66 ppm, correspondingly) of pyrazolopyr-idine moiety, two doublets for H$_{4b}$, H$_{7b}$ (7.54 and 7.75 ppm), the overlapped H$_{5b}$, H$_{6b}$ proton signals in one multiplet (7.24 ppm) for a benzimidazole moiety and two singlet resonances for H$_{1a}$ and H$_{1b}$ (for atom numbering, see Chart 1). The substitution of H$_{5a}$ by bromine (**L2**) results in reduced multiplicity for the H$_{4a}$ and H$_{6a}$ signals (two doublets at 8.99 and 8.75 ppm), whereas the benzi-midazole moiety spectrum remains almost unchanged. Two sing-lets were attributed to NH protons and related to pyrazolopyridine (H$_{1a}$, at 14.19 (**L1**), 14.43 (**L2**) ppm) and benzimidazole (H$_{1b}$, at 13.11 (**L1**), 13.19 (**L2**) ppm) moieties.

NMR spectra for **11a**, **11b**, **12a**, and **12b**, where **L1** and **L2** coordinate as bidentate ligands via N$_{2a}$ and N$_{3b}$ with the formation of a stable five-membered chelate cycle, show one set of signals. There was no evidence for monodentate or tridentate coordination of ligands with the formation of dinuclear or polynuclear complexes.

Coordination of **L1** and **L2** to ruthenium(II) made it possible to assign the two doublets to proton resonances of H$_{4b}$ and H$_{7b}$ of the benzimidazole moiety. In the ^{1}H, ^{1}H ROESY plots, one of them has cross-peaks with a CH cymene ring and the nearest to them is H$_{4b}$ (e.g., at 8.11 (**11a**), 8.06 (**12a**) ppm). A singlet at 14.91 (**11a**), 14.34 (**12a**) ppm was assigned to NH proton and showed no couplings with other atoms. The nitrogen resonance shift at 128.7 (**11a**), 127.3 (**12a**) ppm is closer to the benzimi-dazole NH chemical shift in metal-free ligands (121.3 (**L1**, **L2**) ppm) and, therefore, was assigned as N$_{1b}$ (see Table S3 in the Supporting Information). The H$_{1b}$ resonance shows a significant shift by 1.8 and 1.15 ppm for **11a** and **12a**, respectively, upon ligand coordination (**L1** and **L2**) to the metal(II)-arene moiety.

Scheme 4. Coordination of L3 (7b-L3 (left) and 4b′-L3 (right) Tautomers)

The nearest to the metal binding site pyrazolopyridine proton H_{1a} was not detected for **11a**, **11b**, **12a**, and **12b**, and the proton resonance of H_{1b} was also not seen for **11b** or **12b**.

L3 displays two sets of signals originated from 7b-**L3** and 4b′-**L3** tautomers (see Chart 1). The signals of pyrazolopyridine moieties are partially overlapped (e.g., H_{1a} ($H_{1a'}$) at 14.47 and 14.43 ppm, H_{4a} ($H_{4a'}$) at 8.99 and 8.98 ppm, H_{6a} ($H_{6a'}$) at 8.75 ppm), whereas the signals of the benzimidazole moieties are better resolved (see Table S1 in the Supporting Information).

According to the $^1H,^1H$ ROESY plot, one of the CH_2 groups at 4.80 ppm couples with the N*H* proton at 13.25 ppm, indicating their attribution to the 7b-**L3** tautomer, whereas another N*H* proton at 13.22 ppm gives a cross-peak with $H_{7b'}$ at 7.47 ppm and belongs to 4b′-**L3** tautomer (Figure 1).

Tautomers 7b-**L3** and 4b′-**L3** are present in solution in 1:1.3 molar ratio and give, for the substituted benzimidazole moiety, two singlets ($H_{1b'}$ at 13.22 ppm, H_{1b} at 13.25 ppm), two doublets of doublets ($H_{7b'}$ at 7.47 ppm, H_{4b} at 7.72 ppm), one multiplet (H_{5b}, H_{6b}, $H_{5b'}$, $H_{6b'}$ at 7.28−7.21 ppm), two CH_2 (4.80 (H_{10b}), 4.96 ($H_{10b'}$) ppm) and two CH_3 singlets at 3.37 (H_{11b}) and 3.44 ($H_{11b'}$) ppm. The absence of cross-peaks between $H_{7b'}$ and H_{4b} in the $^1H,^1H$ COSY plot supports their relation to the two different molecules.

The binding site in 4b′-**L3** tautomer is sterically shielded by a methoxymethyl group. Consistent with this NMR spectra display, only one set of signals is shown for **13a** and **13b** with the coordination of the 7b-**L3** tautomer to ruthenium(II) and osmium(II) via N_{2a} and N_{3b} (see Scheme 4).

The preference for coordination of the 7b-**L3** tautomer is also confirmed by $^1H,^1H$ ROESY plots: H_{4b} (7.99 (**13a**), 7.91 (**13b**) ppm) has couplings with CH protons of cymene ring. The cross-peak between H_{10b} at 4.88 ppm (**13a**) and N*H* at 13.88 ppm (**13a**) enabled the assignment of this singlet to a benzimidazole moiety (H_{1b}). In addition, the chemical shifts for the C atoms of the benzimidazole moiety (C_{4b}, C_{7b}, C_{5b}, C_{6b}) of the coordinated ligand and metal-free 7b-**L3** tautomer are very similar (see Table S2 in the Supporting Information). The nitrogen resonance at 122.9 ppm (**13a**) compares well to the benzimidazole N*H* chemical shift in metal-free **L3** at 121.4 ppm. As for **11a**, **11b**, **12a**, and **12b**, the nearest to the coordination place pyrazolopyridine proton H_{1a} resonance was not detected.

According to the $^1H,^1H$ ROESY plots of **11a**, **12a**, **13a**, and **13b** only CH cymene ring protons have couplings with the nearest H_{4b} benzene ring proton, suggesting that the isopropyl or methyl groups are further away from the H_{4b} proton.

Crystal Structures. The results of the XRD studies of $[Os^{II}Cl(\eta^6\text{-}p\text{-cymene})(L1)]Cl\cdot4H_2O$ (**11b**·4H$_2$O), $[Os^{II}Cl(\eta^6\text{-}p\text{-cymene})(L2)]Cl$ (**12b**), $[Os^{II}Cl(\eta^6\text{-}p\text{-cymene})(L2)]Cl\cdot2CH_3OH\cdot2H_2O$ (**12b**·2CH$_3$OH·2H$_2$O), $[Ru^{II}Cl(\eta^6\text{-}p\text{-cymene})(L3−H)]$ (**13c**),
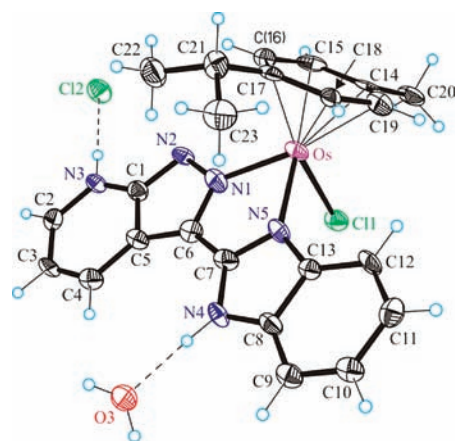

Figure 2. Fragment of the crystal structure of **11b**·4H$_2$O showing nitrogen atoms N3 and N4, which act as proton donors in intermolecular hydrogen bonding interactions N3−H···Cl2 [N3···Cl2 3.067(7) Å, N3−H···Cl2 177.3°] and N4−H···O3 [N4···O3 2.671(9) Å, N4−H···O3 170.9°]; thermal ellipsoids have been drawn at 50% probability level. Selected bond lengths and angles: Os−Cl1, 2.421(2) Å; Os−N1, 2.072(7) Å; Os−N5, 2.096(7) Å; Os−C(arene)$_{av}$, 2.198(32) Å; C1−N2, 1.349(11) Å; N2−N1, 1.366(10) Å; N1−C6, 1.357(11) Å; C6−C7, 1.428(12) Å; C7−N5, 1.345(11) Å; N5−C13, 1.391(11) Å; N1−Os−N5, 75.6(3)°; N1−Os−Cl1, 85.5(2)°; N5−Os−Cl1, 83.4(2)°.
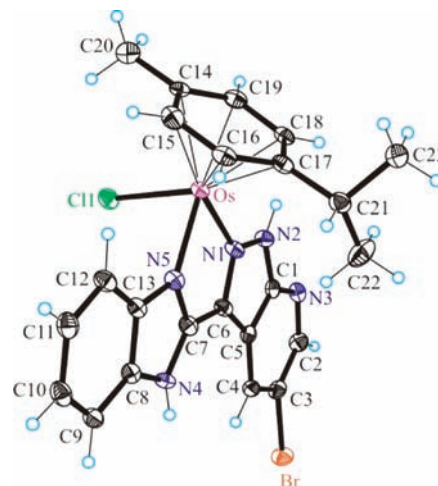
Figure 3. ORTEP plot of the structure of the cation $[Os^{II}Cl(\eta^6\text{-}p\text{-cymene})(L2)]^+$ in **12b**·2CH$_3$OH·2H$_2$O. Thermal ellipsoids have been drawn at the 50% probability level. Selected bond lengths and angles: Os−Cl1, 2.4043(1) Å; Os−N1, 2.083(3) Å; Os−N5, 2.097(3) Å; Os−C(arene)$_{av}$, 2.197(26) Å; C1−N2, 1.361(5) Å; N2−N1, 1.344(4) Å; N1−C6, 1.336(5) Å; C6−C7, 1.447(6) Å; C7−N5, 1.335(5) Å; N5−C13, 1.380(5) Å; N1−Os−N5, 74.73(13)°; N1−Os−Cl1, 84.29(10)°; and N5−Os−Cl1, 83.25(10)°.

$[Ru^{II}Cl(\eta^6\text{-}p\text{-cymene})(L3)]Cl\cdot[Ru^{II}Cl(\eta^6\text{-}p\text{-cymene})(L3−H)]\cdot CH_3OH$ (**13d**·CH$_3$OH) and $[Os^{II}Cl(\eta^6\text{-}p\text{-cymene})(L3)]Cl\cdot[Os^{II}Cl(\eta^6\text{-}p\text{-cymene})(L3−H)]\cdot0.75CH_3OH\cdot0.25H_2O$ (**13e**·0.75CH$_3$OH·0.25H$_2$O) are shown in Figures 2, Figure S2 in the Supporting Information, and Figures 3−6, respectively. All complexes have a typical "three-legged piano-stool" geometry of ruthenium(II) and osmium(II) arene complexes, with an η^6 π-bound p-cymene ring forming the seat and three other donor atoms (two nitrogens N1 and
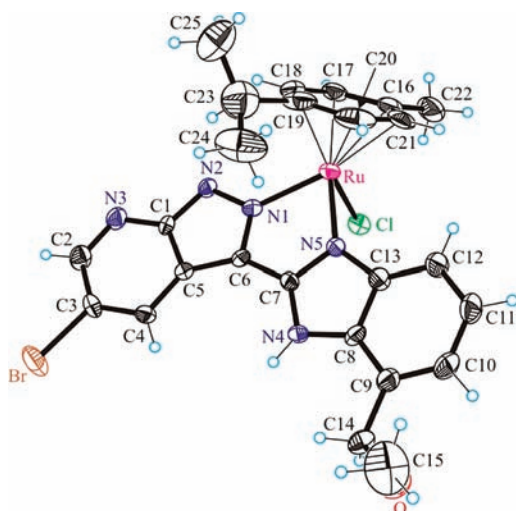
Figure 4. ORTEP plot of the complex $[Ru^{II}Cl(\eta^6\text{-}p\text{-cymene})(L3-H)]$ (**13c**). Thermal ellipsoids have been drawn at 30% probability level. Selected bond lengths and angles: Ru−Cl, 2.399(2) Å; Ru−N1, 2.067(6) Å; Ru−N5, 2.089(5) Å; Ru−C(arene)$_{av}$, 2.186(31) Å; C1−N2, 1.366(8) Å; N2−N1, 1.353(7) Å; N1−C6, 1.362(7) Å; C6−C7, 1.426(9) Å; C7−N5, 1.335(8) Å; N5−C13, 1.398(8) Å; N1−Ru−N5, 75.9(2)°; N1−Ru−Cl, 87.35(17)°; and N5−Ru−Cl, 85.73(17)°.

N5 of the corresponding 3-(1*H*-benzimidazol-2-yl)-1*H*-pyrazolo[3,4-*b*]pyridine and one chlorido ligand) as the legs of the stool. Selected bond distances and angles are quoted in the figure captions. All complexes crystallize as racemates, because of the presence of the stereogenic metal center.

The bidentate 3-(1*H*-benzimidazol-2-yl)-1*H*-pyrazolo[3,4-*b*]-pyridines, which can have different substituents in positions 5a and 7b, reveal different acid−base properties. It can act as a neutral organic ligand, with nitrogen atoms N2 and N4 as proton donors involved in intermolecular hydrogen bonding interactions N4−H···O1^i(−x + 1, −y + 1, −z + 2) [N4···O1^i, 2.730(4) Å; N4−H···O1^i, 176.1°] and N2−H···O3^{ii}(−x + 2, −y + 1, −z + 1 [N2···O3^{ii}, 2.697(4) Å; N4−H···O1^i, 172.3°] with one methanol and one water molecule, respectively, as is the case for **12b**·2CH$_3$OH·2H$_2$O (Figure 3) or N2−H···Cl2-(Cl2X) and N4−H···Cl1^i(−x, −y, −z + 2) [N4···Cl1^i, 3.213(9) Å; N4−H···O1^i, 162.91°] in **12b** (see Figure S2 in the Supporting Information), correspondingly. The ligand can be protonated at N3 (N3−H···Cl2) and deprotonated at N2 [N2···H−O4^i (−x + 1, −y + 1, −z + 1) with N2···O4^i 2.923(9) Å, N2···H−O4^i 138.7°] (overall charge zero) with atom N4 as a proton donor to one of the four co-crystallized water molecules N4−H···O3, as occurs in **11b**·4H$_2$O (see Figure 2).

In **13c**, the ligand was found to be deprotonated at N2, acting as a proton acceptor in the intermolecular hydrogen bonding interaction N2···H−N4^i (i denotes symmetry transformations x, −y + 1.5, z + 0.5) used to generate equivalent atoms) [N2···N4^i, 2.896(7) Å; N2···H−N4^i, 155.6°] (see Figure 4).

Complexes **13d**·CH$_3$OH and **13e**·0.75CH$_3$OH·0.25H$_2$O crystallized both in the centrosymmetric triclinic space group $P\bar{1}$. The asymmetric unit in both consists of a neutral complex $[M^{II}Cl(\eta^6\text{-}p\text{-cymene})(L3-H)]$ and a complex cation $[M^{II}Cl(\eta^6\text{-}p\text{-cymene})(L3)]^+$ (M = Ru or Os), a chloride counteranion and co-crystallized solvent (methanol or methanol/water). Deprotonation of the organic ligand in $[M^{II}Cl(\eta^6\text{-}p\text{-cymene})(L3-H)]$ is
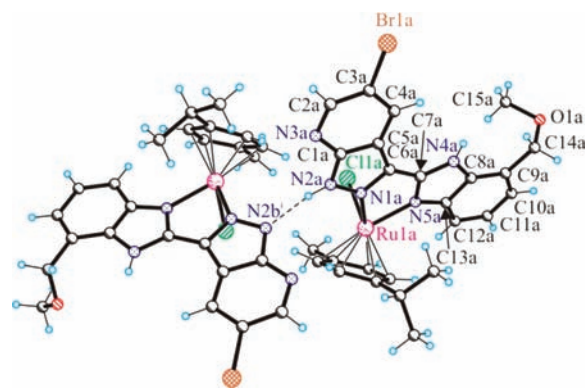
Figure 5. Fragment of the crystal structure of $[Ru^{II}Cl(\eta^6\text{-}p\text{-cymene})\text{-}(L3)]Cl\cdot[Ru^{II}Cl(\eta^6\text{-}p\text{-cymene})(L3-H)]\cdot CH_3OH$ (**13d**·CH$_3$OH) showing the intermolecular hydrogen bonding N2a−H···N2b [N2a···N2b^i (−x + 1, −y + 1, −z + 1), 2.814(7) Å; N2a−H···N2b^i, 163.3°]. Selected bond lengths and angles: Ru1a−Cl1a, 2.3952(17) Å; Ru1a−N1a, 2.078(5) Å; Ru1a−N5a, 2.099(5) Å; Ru1a−C(arene)$_{av}$, 2.194(33) Å; C1a−N2a, 1.358(8) Å; N2a−N1a, 1.354(7) Å; N1a−C6a, 1.350(8) Å; C6a−C7a, 1.441(9) Å; C7a−N5a, 1.335(8) Å; N5a−C13a, 1.381(8) Å; N1a−Ru1a−N5a, 75.6(2)°; N1a−Ru1a−Cl1a, 84.45(15)°; and N5a−Ru1a−Cl1a, 85.05(15)°.
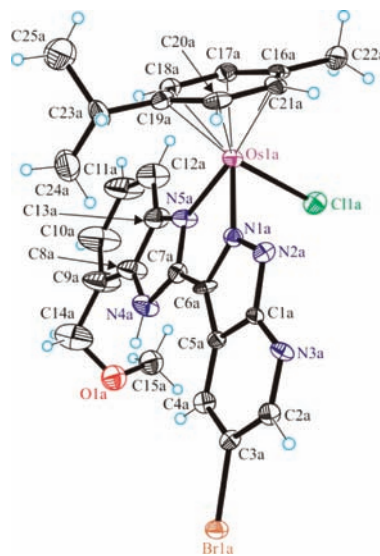
Figure 6. ORTEP plot of $[Os^{II}Cl(\eta^6\text{-}p\text{-cymene})(L3-H)]$ in $[Os^{II}Cl\text{-}(\eta^6\text{-}p\text{-cymene})(L3)]Cl\cdot[Os^{II}Cl(\eta^6\text{-}p\text{-cymene})(L3-H)]\cdot 0.75CH_3OH\cdot 0.25H_2O$ (**13e**·0.75CH$_3$OH·0.25H$_2$O). Thermal ellipsoids have been drawn at the 40% probability level. Selected bond lengths and angles: Os1a−Cl1a, 2.402(2) Å; Os1a−N1a, 2.068(7) Å; Os1a−N5a, 2.086(7) Å; Os1a−C(arene)$_{av}$, 2.192(25) Å; C1a−N2a, 1.349(10) Å; N2a−N1a 1.369(9) Å; N1a−C6a, 1.361(10) Å; C6a−C7a, 1.431(11) Å; C7a−N5a, 1.339(10) Å; N5a−C13a, 1.398(11) Å; N1a−Os1a−N5a, 75.1(3)°; N1a−Os1a−Cl1a, 83.56(18)°; and N5a−Os1a−Cl1a, 84.2(2)°.

corroborated by the presence of hydrogen bonding of the type N2a···H−N2b^i (−x + 1, −y + 1, −z + 1) in the crystal structure of the ruthenium complex **13d**·CH$_3$OH (Figure 5) and a similar interaction N2b···H−N2a^i (x, y + 1, z) [N2b···N2a^i, 2.810(9) Å; N2b···H−N2a^i, 170.1°] in the crystal of the osmium analogue **13e**·0.75CH$_3$OH·0.25H$_2$O. In Figure 6 the structure of $[Os^{II}Cl(\eta^6\text{-}p\text{-cymene})(L3-H)]$ is shown. In both structures,

Table 2. Antiproliferative Activity of Metal-Free Ligands (L1−L3), and Their Ruthenium(II) (11a−13a) and Osmium(II) (11b−13b) Arene Complexes, in Three Human Cancer Cell Lines (CH1, SW480, and A549)[a]

compound	metal	IC$_{50}$ [μM][b]		
		CH1	SW480	A549
L1		11 ± 3	23 ± 6	29 ± 7
11a	Ru	96 ± 18	>320	525 ± 102
11b	Os	64 ± 19	223 ± 29	>640
L2		1.5 ± 0.6	5.1 ± 1.0	6.7 ± 0.3
12a	Ru	21 ± 3	70 ± 8	268 ± 35
12b	Os	22 ± 3	29 ± 2	123 ± 21
L3		0.63 ± 0.09	0.74 ± 0.26	5.2 ± 0.5
13a	Ru	11 ± 1	11 ± 2	68 ± 12
13b	Os	7.9 ± 2.2	12 ± 2	89 ± 11

[a] CH1 denotes ovarian cancer, human; SW480 denotes colon carcinoma, human; and A549 denotes non-small-cell lung carcinoma, human. [b] 50% inhibitory concentrations (mean value $\pm$ standard deviation from at least three independent experiments) obtained by the MTT assay (96-h exposure).

the atoms N4a and N4b act as proton donors in strong hydrogen bonding interactions to the chloride counteranion, namely, N4a$\cdots$H−Cl2^{ii} ($-x + 1, -y + 2, -z + 1$) [N4$\cdots$Cl2^{ii}, 3.275(6) Å; N4a$\cdots$H−Cl2^{ii}, 176.9°], N4b$\cdots$H−Cl2 [N4b$\cdots$Cl2, 3.211(5) Å; N4b$\cdots$H−Cl2, 176.0°] (**13d**·CH$_3$OH) and N4a$\cdots$H−Cl2^{ii} ($-x + 1, -y + 1, -z + 1$) [N4a$\cdots$Cl2^{ii}, 3.273(8) Å; N4a$\cdots$H−Cl2^{ii}, 177.0°], N4b$\cdots$H−Cl2^{ii} [N4b$\cdots$Cl2, 3.204(7) Å; N4b$\cdots$H−Cl2, 177.0°] (**13e**·0.75CH$_3$OH·0.25H$_2$O).

Antiproliferative Activity. Ligands **L1**−**L3**, as well as the corresponding ruthenium(II) (**11a**−**13a**) and osmium(II) (**11b**−**13b**) arene complexes, were studied with regard to their capacity of inhibiting cell growth in vitro in the human cancer cell lines CH1 (ovarian carcinoma), SW480 (colon carcinoma), and A549 (non-small cell lung cancer), yielding the IC$_{50}$ values listed in Table 2. All compounds show the strongest effect in the generally chemosensitive CH1 cells, whereas the more chemoresistant A549 cells are also less affected by the compounds investigated here. The antiproliferative activity of the metal-free ligands decreases in the rank order **L3** > **L2** > **L1**, indicating that bromination (**L2, L3**) and, even more so, the double substitution (bromination and an additional replacement of H by a methoxymethyl group (**L3**)) are advantageous, with regard to activity. These structure−activity relationships are also reflected in the rank orders of the corresponding ruthenium and osmium complexes for the ruthenium complexes, **13a** > **12a** > **11a**, and for the osmium complexes, **13b** > **12b** > **11b**.

However, the IC$_{50}$ values are shifted to higher concentrations (see Figure 7). The differences between the ruthenium and osmium analogues are mostly small (IC$_{50}$ values differ only up to a factor of 2.4), with the osmium complexes being at least as active as their ruthenium counterparts.

Cell Cycle Effects. Since 3-(1*H*-benzimidazol-2-yl)-1*H*-pyrazolo-[3,4-*b*]pyridines have been reported to be potent Cdk inhibitors, we expected the investigated ligands and complexes to induce cell cycle perturbations. To confirm this assumption in a sensitive cell line, exponentially growing CH1 cells were treated with the compounds for 24 h, stained with propidium iodide, and analyzed for their DNA content by fluorescence-activated cell sorting (FACS). Surprisingly,
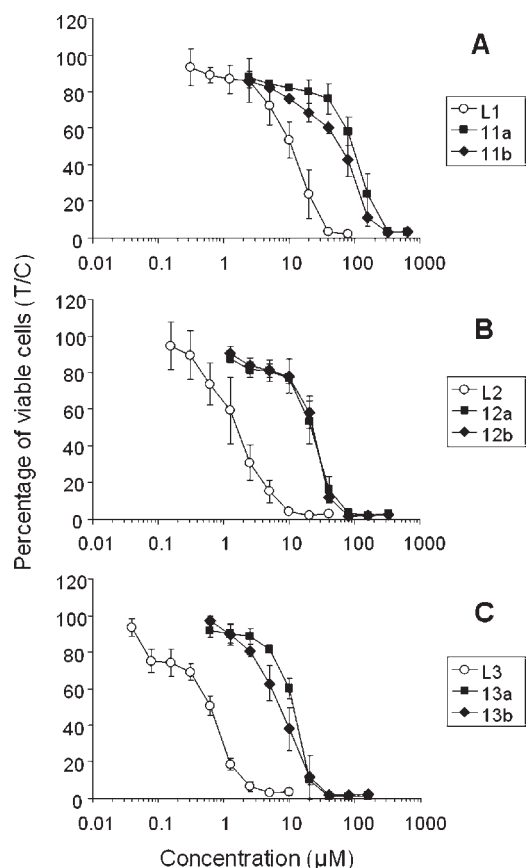

Figure 7. Concentration−effect curves of each ligand, compared to the corresponding ruthenium and osmium complexes, in CH1 ovarian cancer cells (MTT assay, 96 h exposure): (A) **L1, 11a, 11b**; (B) **L2, 12a, 12b**; and (C) **L3, 13a, 13b**. Both the presence of substituents in the ligands and complexation result in a marked shift of antiproliferative activity.

the metal-free ligands **L1**−**L3** turned out to exert only modest effects on cell cycle distribution, with a slight increase of the G2/M fraction from 32% in the untreated control to 53% by 20 μM **L2** as the strongest effect observed in this setting (higher concentrations of this compound led to disintegration of cells already after 24 h). However, the less cytotoxic ruthenium complexes **12a** and **13a**, both bearing substituted ligands (**L2** and **L3** correspondingly), cause a more pronounced G2/M phase arrest, as reflected by an increase of this cell fraction to 65% at 80 μM and 59% at 40 μM, respectively, and a concomitant decrease of the G0/G1 fraction to 21% and 24% (compared to 42% in controls), whereas ruthenium complex **11a** bearing an unsubstituted ligand **L1** is devoid of activity on the cell cycle. On the other hand, the osmium complexes do not generally show stronger effects on the cell cycle than the metal-free ligands, perhaps with the exception of **13b**, which induces an increase of the G2/M fraction up to 53% at 80 μM, accompanied by a decline of the G0/G1 fraction to 31% (see Figure 8).

Cdk-Inhibitory Activity. Although the lack of generally pronounced cell cycle effects does not argue for a strong role of Cdk inhibition in the mechanism of action of the investigated compounds, inhibitory potencies were studied in cell-free experiments with two recombinant Cdk/cyclin complexes, by means of the histone H1 kinase assay. Results reveal that all compounds are capable of inhibiting kinase activities in a concentration-dependent manner, being more effective on Cdk2/cyclin E than
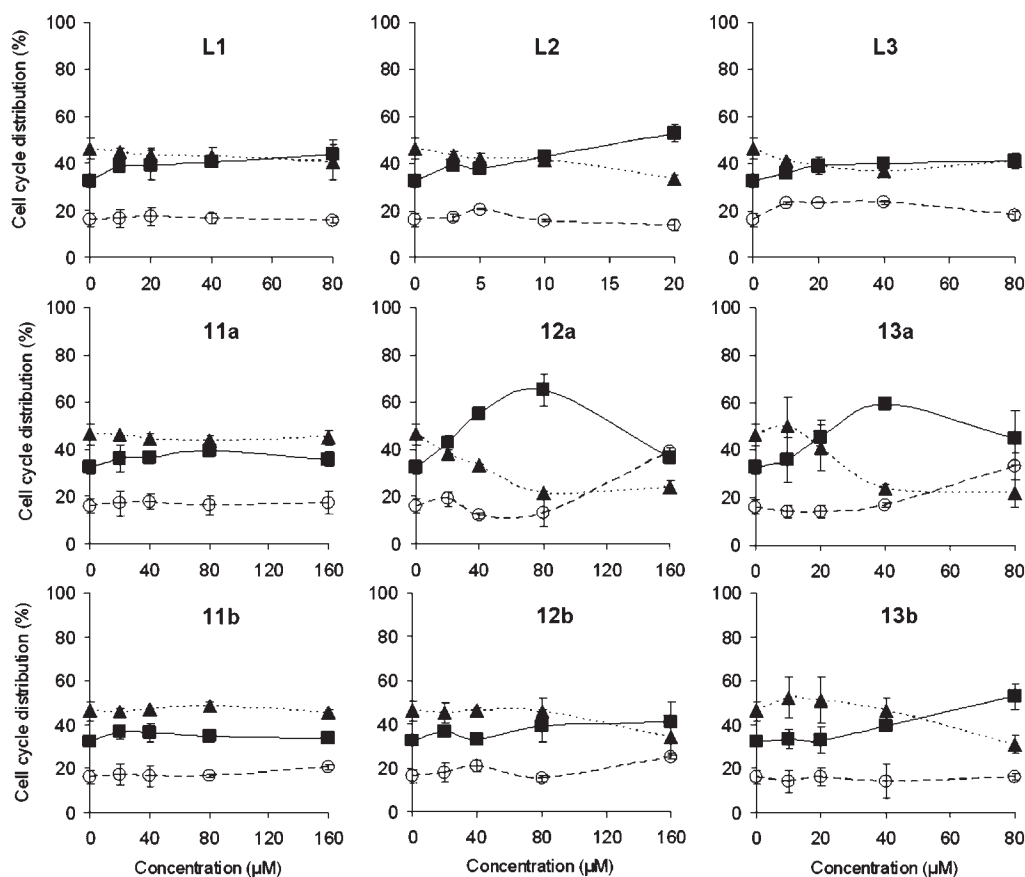
Figure 8. Concentration-dependent effects of metal-free ligands (top), and the corresponding ruthenium (middle) and osmium complexes (bottom), on the cell cycle distribution of CH1 cells ((▲) G0/G1, (○) S, and (■) G2/M phase). Note the different concentration scales.
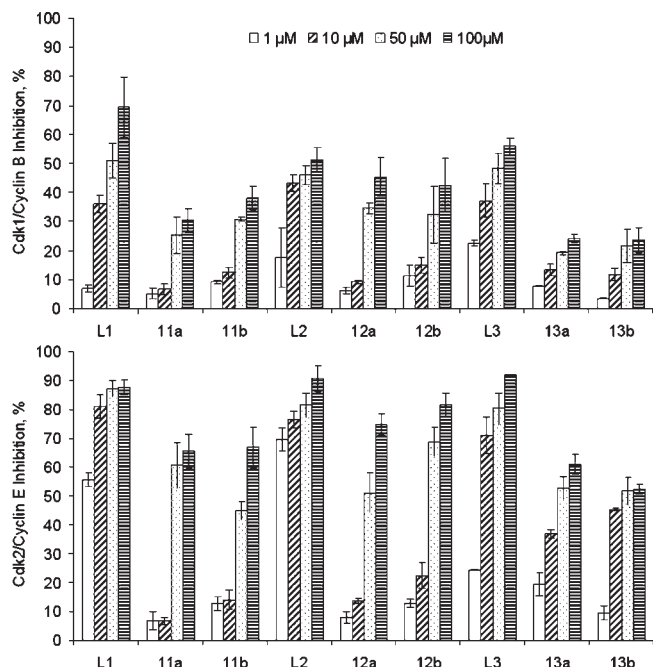
Figure 9. Concentration-dependent effects of metal-free ligands (**L1**–**L3**) as well as corresponding ruthenium (**11a**–**13a**) and osmium complexes (**11b**–**13b**), on kinase activities of recombinant Cdk1/cyclin B (top) and Cdk2/cyclin E (bottom).

on Cdk1/cyclin B (see Figure 9). In contrast to the observed cell cycle effects, but in accordance with antiproliferative activities, Cdk-inhibitory potency of the metal-free ligands is consistently higher than that of the metal complexes. In particular, only **L1**–**L3** effectively inhibit Cdk2/cyclin E in low concentrations (1 μM or 10 μM), whereas all complexes require higher concentrations to exert >50% inhibitory effects. As in the MTT assay, differences between the effects of corresponding ruthenium and osmium complexes are minor, compared to the differences from those of the metal-free ligands.

■ CONCLUSION

The known multistep synthesis of 3-(1*H*-benzimidazol-2-yl)-1*H*-pyrazolo[3,4-*b*]pyridines, which we have modified, essentially afforded three organic compounds (**L1**–**L3**) that possess Cdk-inhibiting properties. These were used as bidentate ligands, and six novel organometallic complexes of the general formula [M^{II}Cl(η^6-*p*-cymene)(L)]Cl, where M = Ru (**11a**, **12a**, **13a**) or Os (**11b**, **12b**, **13b**) and L = **L1**–**L3**, have been synthesized and comprehensively characterized using spectroscopic and X-ray diffraction methods. Complexation of **L1**–**L3** with ruthenium or osmium yielded compounds with increased solubility in the biological medium, yet lowered antiproliferative activity in human cancer cell lines. Modulation of biological activities by substitution at the ligands can be accomplished in the metal-free molecules and their metal complexes in a similar way. The known Cdk-inhibitory activity of the ligands could be confirmed in cell-

free experiments, in particular in Cdk2/cyclin E, and their stronger effects on Cdk activity parallel their higher capacity of inhibiting cancer cell growth in vitro, compared to their metal complexes. Nevertheless, the lack of pronounced effects on the cell cycle of chemosensitive ovarian cancer cells argues against a major role for inhibition of cell growth, at least in this setting.

■ ASSOCIATED CONTENT

Ⓢ Supporting Information. Assigned NMR (^{1}H, ^{13}C, ^{15}N) signals for **L1**–**L3**, **11a**–**13a**, **11b**–**13b** (Tables S1–S3); ORTEP plot of 5-bromo-3-methyl-1H-pyrazolo[3,4-b]pyridine in **2**·0.5H$_2$O (Figure S1); ORTEP plot of [Os^{II}Cl(η^6-p-cymene)-(**L2**)]$^+$ in **12b** (Figure S2); stability of complexes in solution; time-dependent UV–vis spectra of **L1**, **11a**, and **11b** in MeOH (Figure S3); time-dependent UV–vis spectra of **L3**, **13a**, and **13b** in MeOH (Figure S4); time-dependent UV–vis spectra of **11a** in H$_2$O for 48 h (Figure S5); crystallographic data for **2**·0.5H$_2$O, **11b**·4H$_2$O, **12b**, **12b**·2CH$_3$OH·2H$_2$O, **13c**, **13d**·CH$_3$OH, and **13e**·0.75CH$_3$OH·0.25H$_2$O (in CIF format). This material is available free of charge via the Internet at http://pubs.acs.org.

■ AUTHOR INFORMATION

Corresponding Author
*E-mail addresses: vladimir.arion@univie.ac.at (V.B.A.); bernhard. keppler@univie.ac.at (B.K.K.).

■ ACKNOWLEDGMENT

■ REFERENCES

(1) Malumbres, M.; Barbacid, M. *Nat. Rev. Cancer* **2009**, *9*, 153–166.

(2) Senderowicz, A. M. *Oncogene* **2003**, *22*, 6609–6620.

(3) Shapiro, G. I. *J. Clin. Oncol.* **2006**, *24*, 1770–1783.

(4) Harper, J. W.; Adams, P. D. *Chem. Rev.* **2001**, *101*, 2511–2526.

(5) Malumbres, M.; Pevarello, P.; Barbacid, M.; Bischoff, J. R. *Trends Pharmacol. Sci.* **2008**, *29*, 16–21.

(6) Bible, K. C.; Kaufmann, S. H. *Cancer Res.* **1997**, *57*, 3375–3380.

(7) Bible, K. C.; Boerner, S. A.; Kirkland, K.; Anderl, K. L.; Bartelt, D., Jr.; Svingen, P. A.; Kottke, T. J.; Lee, Y. K.; Eckdahl, S.; Stalboerger, P. G.; Jenkins, R. B.; Kaufmann, S. H. *Clin. Cancer Res.* **2000**, *6*, 661–670.

(8) Bible, K. C.; Lensing, J. L.; Nelson, S. A.; Lee, Y. K.; Reid, J. M.; Ames, M. M.; Isham, C. R.; Piens, J.; Rubin, S. L.; Rubin, J.; Kaufmann, S. H.; Atherton, P. J.; Sloan, J. A.; Daiss, M. K.; Adjei, A. A.; Erlichman, C. *Clin. Cancer Res.* **2005**, *11*, 5935–5941.

(9) Coley, H. M.; Shotton, C. F.; Kokkinos, M. I.; Thomas, H. *Gynecol. Oncol.* **2007**, *105*, 462–469.

(10) Travnicek, Z.; Popa, I.; Cajan, M.; Herchel, R.; Marek, J. *Polyhedron* **2007**, *26*, 5271–5282.

(11) Malon, M.; Travnicek, Z.; Marysko, M.; Zboril, R.; Maslan, M.; Marek, J.; Dolezal, K.; Rolcik, J.; Krystof, V.; Strnad, M. *Inorg. Chim. Acta* **2001**, *323*, 119–129.

(12) Dvorak, L.; Popa, I.; Starha, P.; Travnicek, Z. *Eur. J. Inorg. Chem.* **2010**, 3441–3448.

(13) Travnicek, Z.; Popa, I.; Cajan, M.; Zboril, R.; Krystof, V.; Mikulik, J. *J. Inorg. Biochem.* **2010**, *104*, 405–417.

(14) Primik, M. F.; Muehlgassner, G.; Jakupec, M. A.; Zava, O.; Dyson, P. J.; Arion, V. B.; Keppler, B. K. *Inorg. Chem.* **2010**, *49*, 302–311.

(15) Ginzinger, W.; Arion, V. B.; Giester, G.; Galanski, M.; Keppler, B. K. *Centr. Eur. J. Chem.* **2008**, *6*, 340–346.

(16) Schmid, W. F.; John, R. O.; Arion, V. B.; Jakupec, M. A.; Keppler, B. K. *Organometallics* **2007**, *26*, 6643–6652.

(17) Schmid, W. F.; John, R. O.; Muehlgassner, G.; Heffeter, P.; Jakupec, M. A.; Galanski, M.; Berger, W.; Arion, V. B.; Keppler, B. K. *J. Med. Chem.* **2007**, *50*, 6343–6355.

(18) Schmid, W. F.; Zorbas-Seifried, S.; John, R. O.; Arion, V. B.; Jakupec, M. A.; Roller, A.; Galanski, M.; Chiorescu, I.; Zorbas, H.; Keppler, B. K. *Inorg. Chem.* **2007**, *46*, 3645–3656.

(19) Dobrov, A.; Arion, V. B.; Kandler, N.; Ginzinger, W.; Jakupec, M. A.; Rufinska, A.; Graf von Keyserlingk, N.; Galanski, M.; Kowol, C.; Keppler, B. K. *Inorg. Chem.* **2006**, *45*, 1945–1950.

(20) Filak, L. K.; Muehlgassner, G.; Jakupec, M. A.; Heffeter, P.; Berger, W.; Arion, V. B.; Keppler, B. K. *J. Biol. Inorg. Chem.* **2010**, *15*, 903–918.

(21) Lin, R.; Connolly, P. J.; Lu, Y.; Chiu, G.; Li, S.; Yu, Y.; Huang, S.; Li, X.; Emanuel, S. L.; Middleton, S. A.; Gruninger, R. H.; Adams, M.; Fuentes-Pesquera, A. R.; Greenberger, L. M. *Bioorg. Med. Chem. Lett.* **2007**, *17*, 4297–4302.

(22) Huang, S.; Lin, R.; Yu, Y.; Lu, Y.; Connolly, P. J.; Chiu, G.; Li, S.; Emanuel, S. L.; Middleton, S. A. *Bioorg. Med. Chem. Lett.* **2007**, *17*, 1243–1245.

(23) Chiu, G.; Li, S.; Connolly, P. J.; Middleton, S. A.; Emanuel, S. L.; Huang, S.; Lin, R.; Lu, Y. *PCT Int. Appl.*, WO 2006130673, 2006, 162 pp.

(24) Lin, R.; Chiu, G.; Yu, Y.; Connolly, P. J.; Li, S.; Lu, Y.; Adams, M.; Fuentes-Pesquera, A. R.; Emanuel, S. L.; Greenberger, L. M. *Bioorg. Med. Chem. Lett.* **2007**, *17*, 4557–4561.

(25) Chiu, G.; Yu, Y.; Lin, R.; Li, S.; Connolly, P. J. *PCT Int. Appl.*, WO 2008048502, 2008, 43 pp.

(26) Yu, Y.; Lin, R.; Connolly, P. J. *PCT Int. Appl.*, WO 2008048503, 2008, 42 pp.

(27) Peacock, A. F. A.; Sadler, P. J. *Chem.-Asian J.* **2008**, *3*, 1890–1899.

(28) Bruijnincx, P. C. A.; Sadler, P. J. *Adv. Inorg. Chem.* **2009**, *61*, 1–62.

(29) Hartinger, C. G.; Dyson, P. J. *Chem. Soc. Rev.* **2009**, *38*, 391–401.

(30) Dougan, S. J.; Sadler, P. J. *Chimia* **2007**, *61*, 704–715.

(31) Ang, W. H.; Dyson, P. J. *Eur. J. Inorg. Chem.* **2006**, 4003–4018.

(32) Dyson, P. J. *Chimia* **2007**, *61*, 698–703.

(33) Kuo, D. L. *Tetrahedron* **1992**, *48*, 9233–9236.

(34) Lynch, B. M.; Khan, M. A.; Teo, H. C.; Pedrotti, F. *Can. J. Chem.* **1988**, *66*, 420–428.

(35) Georg, G. I.; Tash, J. S.; Chakrasali, R.; Jakkaraj, S. R. *PCT Int. Appl.*, WO 2006023704, 2006, 182 pp.

(36) Berdini, V.; O'Brien, M. A.; Carr, M. G.; Early, T. R.; Navarro, E. F.; Gill, A. L.; Howard, S.; Trewartha, G.; Woolford, A. J.-A.; Woodhead, A. J.; Wyatt, P. *PCT Int. Appl.*, WO 2005002552, 2005, 287 pp.

(37) Bennett, M. A.; Smith, A. K. *J. Chem. Soc., Dalton Trans.* **1974**, 233–241.

(38) Kiel, W. A.; Ball, R. G.; Graham, W. A. G. *J. Organomet. Chem.* **1990**, *383*, 481–496.

(39) *SAINT-Plus*, version 7.06a and APEX2; Bruker–Nonius AXS, Inc.: Madison, WI, 2004.

(40) Sheldrick, G. M. *Acta Crystallogr., Sect. A: Found. Crystallogr.* **2008**, *A64*, 112–122.

(41) Burnett, M. N.; Johnson, G. K. *ORTEPIII*, Report ORNL-6895; Oak Ridge National Laboratory; Oak Ridge, TN, 1996.

(42) Marko, D.; Schätzle, S.; Friedel, A.; Genzlinger, A.; Zankl, H.; Meijer, L.; Eisenbrand, G. *Br. J. Cancer* **2001**, *84*, 283–289.

(43) Zeng, Q.; Yao, G.; Wohlhieter, G. E.; Viswanadhan, V. N.; Tasker, A.; Rider, J. T.; Monenschein, H.; Dominguez, C.; Bourbeau, M. P. *PCT Int. Appl.*, WO 2006044860, 2006, 61 pp.

(44) Cui, J. J.; Deal, J. G.; Gu, D.; Guo, C.; Johnson, M. C.; Kania, R. S.; Kephart, S. E.; Linton, M. A.; McApline, I. J.; Pairish, M. A.; Palmer, C. L. *PCT Int. Appl.*, WO 2009016460, 2009, 168 pp.

(45) Kenda, B.; Quesnel, Y.; Ates, A.; Michel, P.; Turet, L.; Mercier, J. *PCT Int. Appl.*, WO 2006128693, 2006, 258 pp.

11728

dx.doi.org/10.1021/ic201704u |*Inorg. Chem.* 2011, 50, 11715–11728